ORIGINAL RESEARCH

American Heart Association | American Stroke Association

A Critical Role for the Vascular Endothelium in Functional Neurovascular Coupling in the Brain

Brenda R. Chen, PhD; Mariel G. Kozberg, MPhil; Matthew B. Bouchard, PhD; Mohammed A. Shaik, BS; Elizabeth M. C. Hillman, PhD

***Background*—**The functional modulation of blood flow in the brain is critical for brain health and is the basis of contrast in functional magnetic resonance imaging. There is evident coupling between increases in neuronal activity and increases in local blood flow; however, many aspects of this neurovascular coupling remain unexplained by current models. Based on the rapid dilation of distant pial arteries during cortical functional hyperemia, we hypothesized that endothelial signaling may play a key role in the long-range propagation of vasodilation during functional hyperemia in the brain. Although well characterized in the peripheral vasculature, endothelial involvement in functional neurovascular coupling has not been demonstrated.

***Methods and Results*—**We combined in vivo exposed-cortex multispectral optical intrinsic signal imaging (MS-OISI) with a novel in vivo implementation of the light-dye technique to record the cortical hemodynamic response to somatosensory stimulus in rats before and after spatially selective endothelial disruption. We demonstrate that discrete interruption of endothelial signaling halts propagation of stimulus-evoked vasodilation in pial arteries, and that wide-field endothelial disruption in pial arteries significantly attenuates the hemodynamic response to stimulus, particularly the early, rapid increase and peak in hyperemia.

***Conclusions*—**Involvement of endothelial pathways in functional neurovascular coupling provides new explanations for the spatial and temporal features of the hemodynamic response to stimulus and could explain previous results that were interpreted as evidence for astrocyte-mediated control of functional hyperemia. Our results unify many aspects of blood flow regulation in the brain and body and prompt new investigation of direct links between systemic cardiovascular disease and neural deficits. **(*J Am Heart Assoc*. 2014;3:e000787 doi: 10.1161/JAHA.114.000787)**

Key Words: endothelial hyperpolarization • functional magnetic resonance imaging • neurovascular coupling • optical imaging • vascular endothelial function • vascular reactivity

Increases in local blood flow almost always accompany stimulus-evoked neuronal activity in the cerebral cortex. These actively mediated increases in blood flow cause an inflow of oxygenated blood that exceeds oxygen consumption. The resulting decrease in the local concentration of (paramagnetic) deoxygenated hemoglobin is the basis of contrast in functional magnetic resonance imaging (fMRI).[1] Identifying the mechanisms driving neuronally coupled blood flow modulations in the brain is thus central to interpretation of fMRI data in both the healthy and diseased brain.[2,3] Moreover, understanding neurovascular coupling is also fundamental to understanding brain physiology and the way in which the brain manages its energy demands. Evidence is building for a connection between impaired neurovascular coupling and neurodegeneration.[4–6] A more complete understanding of the mechanisms of neurovascular coupling could potentially lead to new diagnostic and therapeutic approaches to a range of neurological conditions.

It has become widely accepted that the control of functional hyperemia in the brain employs a specialized mechanism compared to the rest of the body.[7,8] However, despite a range of studies exploring the potential role of astrocytes, pericytes, neurons, and interneurons in neurovascular coupling, a cohesive and consistent model has yet to emerge.[6,7,9–13] The prevailing assumption is that astrocytes, sensing neuronal activity through metabotropic glutamate receptors,[14] release arachidonic acid derivatives onto the smooth muscle cells of penetrating arterioles.[9] However, recent studies have begun to directly challenge the involvement of astrocytes in neurovascular coupling.[11,15,16] In particular, it has been difficult to reconcile the physical distribution, connectivity, and timing of intracellular calcium

From the Laboratory for Functional Optical Imaging, Departments of Biomedical Engineering and Radiology, Columbia University, New York, NY.

Accompanying Data S1 through S6 are available at http://jaha.ahajournals.org/content/3/3/e000787/suppl/DC1

Correspondence to: Elizabeth M.C. Hillman, PhD, 351 Engineering Terrace, 1210 Amsterdam Ave, New York, NY 10027. E-mail: eh2245@columbia.edu

Received April 5, 2014; accepted May 8, 2014.

increases of astrocytes with the spatiotemporal properties of vasodilation during functional hyperemia.[15,17,18]

The role of the vascular endothelium in blood flow modulation is well characterized in the peripheral vasculature,[8,19–22] particularly the ability of the endothelium to propagate vasodilation. Earlier studies using pharmacological stimuli, such as acetylcholine (ACh), in both the in vivo brain[23,24] and in isolated vessels[25,26] have demonstrated the presence of endothelial reactivity and propagation of vasodilation in the cortical vasculature. However, the assumed role of astrocytes in functional coupling in the brain has led to few to consider the potentially important role of the vascular endothelium in functional neurovascular coupling.[7,27,28] Our previous studies benchmarking the timing, pattern, and spatial range of arterial vasodilation during functional hyperemia[18] found a close match to the properties of endothelial signaling pathways,[22] leading us to hypothesize that the endothelium might play a critical role during functional hyperemia. As described further in the Discussion, establishing the involvement of the vascular endothelium in the process of neurovascular coupling is important, because it can provide explanations for many previous results that have been interpreted as evidence for, and against, other neurovascular mechanisms[7,9,15,29] and could have wider implications for understanding neurovascular impairment. Re-evaluating earlier works, we find that no previous studies have specifically assessed whether endothelial mechanisms contribute to normal, cortical functional hyperemia in response to normal, physiological stimulation in the in vivo brain.

In this study, we disrupt the vascular endothelium of cerebral arteries in vivo and demonstrate that this disruption halts retrograde propagation of vasodilation during stimulus-evoked functional hyperemia. We further show that wide-field disruption of the endothelium of superficial arteries can profoundly alter functional hemodynamics in the cortex. These findings suggest that the vascular endothelium is a critical component of the functional hemodynamic response to somatosensory stimulus in the living brain.

Methods

Our overall experimental approach was to selectively disrupt the vascular endothelium of cortical arterioles in the intact, living rat brain and assess the effects of this disruption on the cortical hemodynamic response to sensory stimulation. All animal procedures were reviewed and approved by the Columbia University Institutional Animal Care and Use Committee.

Animal Preparation and Optical Recording of Stimulus-Evoked Hemodynamics

The cortical hemodynamic response to electrical hindpaw stimulation was recorded using multispectral optical intrinsic signal imaging (MS-OISI), an established technique used for assessment of functional hemodynamics in exposed-cortex in vivo models.[1,18,30] Preparatory surgery was performed under isoflurane anesthesia (2% to 3% inhalation in 3:1 air/oxygen mix) and included placement of a tracheotomy for ventilation (TOPO, Kent Scientific, Torrington, CT) and left femoral artery and vein cannulation for continuous blood pressure monitoring (BP1; World Precision Instruments Inc., Sarasota, FL) and drug/dye delivery. A $\approx$3 mm$\times$5 mm region of the rat somatosensory cortex was then exposed by craniotomy, the fourth ventricle was opened to relieve intracranial pressure, and the dura overlying the exposed region was then removed. Dental acrylic (Acraweld; Henry Schein, Dublin OH) was used to seal a glass coverslip with a drop of 1.5% agarose in artificial cerebrospinal fluid (aCSF) over the exposed region, creating a window for imaging while minimizing brain motion and contamination (aCSF: 125 mmol/L of NaCl, 5 mmol/L of KCl, 4.1 mmol/L of $CaCl_2$, 10 mmol/L of glucose, 2.8 mmol/L of MgCl, and 10 mmol/L of HEPES). For imaging, animals were removed from isoflurane and anesthetized by intravenous alpha-chloralose (40 mg/kg^{-1}/h^{-1}). To rule out anesthetic-dependent effects, intraperitoneal urethane anesthesia (1.5 mg/g) was used for both surgery and imaging in a subset of controls. The animal's core body temperature was measured and maintained throughout at 37°C with a rectal thermometer attached to a homoeothermic heating pad (Stoelting Co., Wood Dale, IL). In animals where electrophysiology was performed, a thin silicone sheet (gloss/gloss; Specialty Manufacturing, Inc., Saginaw, MI) was used instead of a glass coverslip to allow insertion of a recording electrode through the window. Stimulation electrodes were placed on the right hindpaw and connected to an electrical stimulation isolation unit (A365; World Precision Instruments Inc.) delivering 0.3-ms pulses at 3 Hz with 1.0 $\pm$ 0.1 mA amplitude under computer control.

MS-OISI employs a camera to capture high-speed images of the cortex.[30] Image sequences were acquired using our home-built MS-OISI system consisting of a Dalsa 1M60 camera and synchronized, filtered light-emitting diodes (LEDs) for strobed illumination.[30] Data were acquired using red (630 nm centered, M625L2; Thorlabs, Inc., Newton, NJ) and green (530 nm centered, M530L2; Thorlabs) LEDs with a 534/43 nm filter in front of the green LED (NT67-031; Edmund Optics Inc., Barrington, NJ). Dual-wavelength data were acquired at 74 frames per second (fps; equivalent to 37 fps for each LED) with a 5-ms exposure time and 512$\times$512 pixel resolution. Each imaging "run" lasted 40 seconds and consisted of 6 seconds of prestimulation, 12 or 2 seconds of stimulation, and 22 or 32 seconds of poststimulation, respectively. Runs were typically acquired in sets of 5 sequential repetitions. Sensory-evoked hemodynamic responses were recorded before and after light-dye disruption. A 496 nm long-pass emission filter (FF01-496/LP-25; Semrock, Inc., Rochester, NY) was placed in

front of the CCD camera to allow fluorescent imaging of the dextran-conjugated fluorescein isothiocyanate (FITC-dx) during blue light illumination. Negligible absorption of green LED light was found for FITC-dx at in vivo concentrations.

In Vivo Light-Dye Disruption of the Cortical Vascular Endothelium and Controls

Used widely in studies of endothelial propagation of vasodilation in the peripheral vasculature, light-dye treatment involves filling a vessel with a fluorescent dye, in our case FITC-dx, and illuminating with bright light at the dye's excitation wavelength. The reactive oxygen species generated by this illumination induce highly localized disruption of the vessel's endothelial cell (EC) membranes, interrupting their ability to conduct signals while leaving the rest of the vessel and smooth muscle cells intact and functioning.[22,24,31,32] Here, we implemented the light-dye method in 2 ways: first, using a fine focused line of laser light to transect signaling within the endothelium of a pial artery that had been observed to dilate in response to stimulation in pre-light-dye recordings. In a second cohort, a larger wide-field area of the pial surface was illuminated to attempt to disrupt the endothelium of all pial arteries previously observed to dilate in response to stimulus.

Parameters for in vivo light-dye treatment were carefully determined in preliminary experiments. For the data shown, following acquisition of pre-light-dye stimulation runs, rats were slowly injected with 0.5 mL of 10% FITC-dx (molecular weight, 70 kDa; 46945; Sigma-Aldrich, St. Louis, MO) in saline through the femoral vein catheter (≈1.2 mL/h). After equilibration and acquisition of control "dye-only" stimulus runs, the endothelium was disrupted by exciting the dye for a period of 6 to 7 minutes with either (1) 488 nm light from a single-mode, fiber-coupled, solid-state, continuous-wave laser (laser 85BCD-030-115 [Melles Griot Light Sources Group, barlsbad, CA] and fiber P3-460A-FC-10 [Thorlabs]) focused using a 50-mm focal-length cylindrical lens (LJ1695RM-A; Thorlabs) to generate a light line 50 to 100 microns wide and 2.5 mm long before tissue scattering (total power, ≈2 to 3 mW) or (2) 470 nm-centered blue light from a 400-μm optical fiber coupled to a high-power LED (M470F1; Thorlabs) focused to a ≈1-mm-diameter spot (before scattering) with ≈6 mW/mm^2 for wide-field treatment. Analysis of the likely penetration depth of these 2 illumination configurations is included in Data S1. In each rat, control runs during somatosensory stimulation were acquired before injection of FITC-dx with blue light illumination of the cortex only, as well as after FITC-dx injection prior to combined blue light illumination.

Further control measurements were performed in each light-dye–treated rat after completion of stimulus-evoked data acquisition to ensure that only the vascular endothelium had been disrupted.[22,24,32,33] These controls included imaging (without stimulation) during cortical application of ACh (0.1 mmol/L), to test for the presence (or lack) of endothelium-dependent vasodilation in untreated and treated regions, and during cortical application of sodium nitroprusside (SNP; 0.1 μmol/L) to test that arterial smooth muscle cells were still responsive in all regions. In each case, the cranial window was removed and an acrylic well was built around the exposed region of the cortex and then filled with either ACh or SNP. A field of view containing both light-dye–treated and nontreated vessels was then imaged for 1 minute after application of ACh or SNP. After each imaging run, the brain was flushed with aCSF and allowed to return to baseline for 15 minutes. Control and treatment area dilations were assessed in arteries of similar resting diameter. Only vessels that exhibited intact smooth muscle–dependent dilation to SNP, but not endothelial-dependent dilation to ACh, were included in analysis. In additional experiments, ACh (1 to 2 μmol/L) was used to isolate the effects of arterial predilation on functional hyperemia to rule out the possible influence of light-dye–induced dilation.

Electrophysiology measurements were performed to ensure that wide-field light-dye treatment did not alter the neuronal response to somatosensory stimulation. A tungsten microelectrode (0.005-mm diameter, 0.5 MΩ; A-M Systems, Sequim, WA) mounted on a micromanipulator was stereotaxically inserted into the cortex to a depth of ≈400 to 500 μm in the center of the responding region identified through initial MS-OISI imaging. Electrode signals were recorded using Spike2 software (Cambridge Electronic Design Limited, Cambridge, UK). Local field potential (LFP) signals were filtered (0.1 to 100 Hz) and processed using MATLAB (The MathWorks, Inc., Natick, MA).

Data Processing

The dynamic dilation and constriction of vessels on the pial surface can be resolved from raw MS-OISI images, whereas light absorption by blood in vessels, including deeper capillary beds, provides a measure of parenchymal hyperemia (corresponding to a superficially weighted sum of contributions from deeper layers[34]; see Data S2). By synchronously illuminating the cortex with different interlaced wavelengths of light, the oxygenation-dependent absorption of light by blood permits mapping of the relative changes in oxy-, deoxy- and total hemoglobin (Δ[HbO], Δ[HbR], and Δ[HbT])[1,18,30] (calculated here from 630 and 530 nm reflectance data using the modified Beer Lambert law with wavelength-dependent path-length factors calculated using Monte Carlo simulations[1,35]). Data were analyzed by averaging responses over repeated identical stimulation runs. Data were temporally filtered at 5 Hz and affine coregistered where necessary. Time

courses were averaged over pixel regions indicated. Vessel diameters were calculated as the full width of the vessel profile on raw 530 nm reflectance data. Vessels examined for diameter measurements were roughly the same resting size (same degree of branching). Functional response maps represent stimulus-evoked changes over the full field of view.

In the data presented here, we primarily focus on ΔHbT as a measure of physical vascular actuation and hyperemia, rather than HbO and HbR dynamics, which combine the effects of vessel volume and oxygenation changes and are influenced by both blood flow changes and oxygen consumption.

Statistical Analysis

Raw data consists of time series of images acquired over multiple repetitions of the stimulation paradigm or, in some cases, pharmacological trials. Parameters are extracted from different locations within the image time series, for multiple repetitions of stimulation, and under different conditions (such as pre- and post-light-dye treatment). Unless otherwise specified, 5 individual stimulus runs were averaged to construct a single data point. This was necessary, for example, in vessel diameter calculations, to ensure sufficient image signal to noise for accurate parameter calculation. Where multiple assessments within a single rat are used, standard errors (SEs) were corrected to account for intraclass correlation. All statistical comparisons are 2-sided *t* tests using Student *t* distribution. Inspection of residuals (eg, through quantile comparisons) indicate that residuals are approximately normally distributed and thus that Student *t* distribution is appropriate. Randomization was not possible for pre- and post-light-dye studies, because the light-dye effect is irreversible, although controls were performed to ensure that light exposure, dye exposure, and time alone were insufficient to generate the effects observed.

Results

Properties of Cortical Functional Hyperemia With Intact Vascular Endothelium

Figure 1a illustrates the vascular organization of the cerebral cortex, with deeper capillary beds fed by perpendicularly

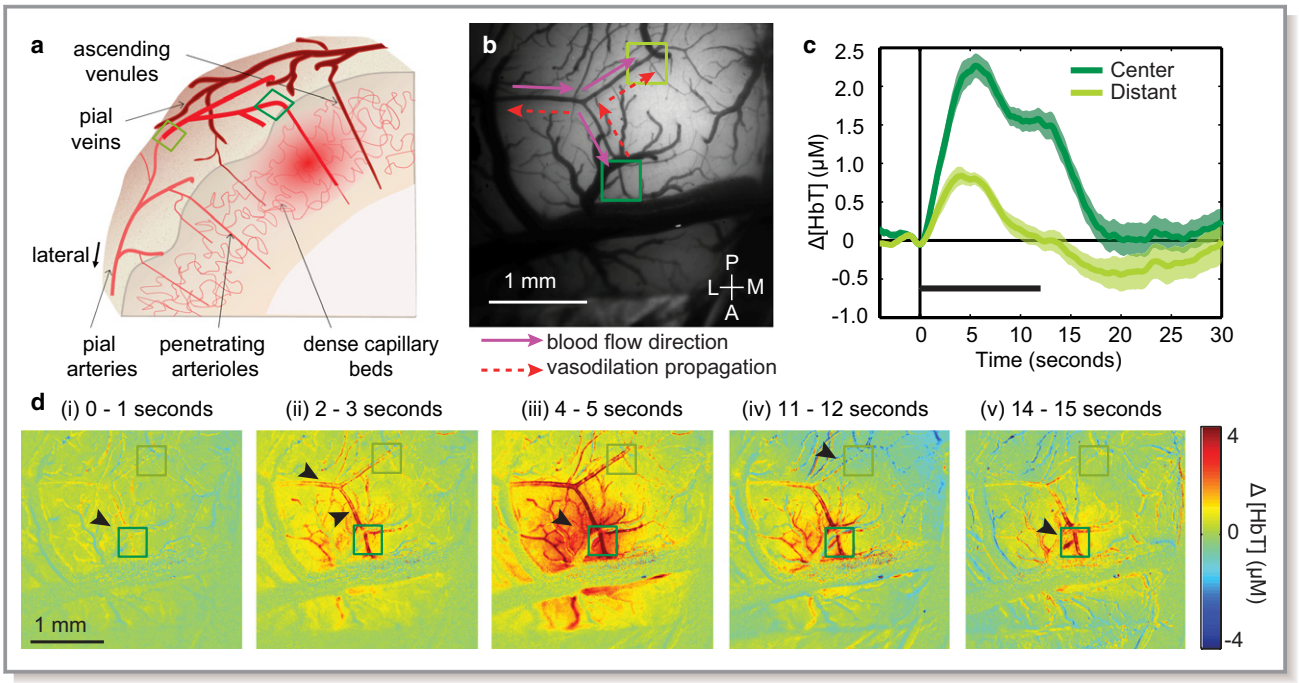

Figure 1. Normal spatiotemporal evolution of the hemodynamic response to somatosensory stimulation. a, Vascular organization of the cerebral cortex. Envisaged capillary hyperemia and retrograde dilation of penetrating arterioles and pial arteries feeding the active region is overlaid in red. b, Grayscale image of the exposed somatosensory cortical surface under 534 nm-centered illumination with arrows indicating direction of blood flow (purple) and propagated vasodilation (red dash). c, Time courses of change in total hemoglobin (Δ[HbT]) extracted from regions of interest indicated in (a), (b) and (d) (average and SEM of N=10 repeated stimulus runs, same rat as in [b] and [d], and in Figure 3a through 3d). d (i through v), Time series of functional maps of Δ[HbT] after onset (at t=0) of 12-second, 3-Hz electrical hindpaw stimulation (same rat and field of view as in [b], averaged over times indicated, average of N=5 repeated stimulus runs). ΔHbT contrast shows both parenchymal hyperemia and the dilation of specific pial arteries. Arrowheads point to features described in the text. A indicates anterior; L, lateral; M, medial; P, posterior.

oriented penetrating arterioles that branch from superficial pial arteries. Figure 1b shows a grayscale image of the exposed somatosensory cortex, with arrows along one of the main feeding arteries indicating both the direction of blood flow and anticipated direction of propagated vasodilation. Figure 1di through 1dv shows an MS-OISI Δ[HbT] time series of the same field of view during a 12-second, 3-Hz electrical hindpaw stimulus. This sequence demonstrates the typical spatiotemporal evolution of the cortical hemodynamic response to stimulation: (i) Slight capillary hyperemia is visible as enhanced ΔHbT contrast in the parenchyma before pial arteries are seen to dilate (ii).[1,18,36,37] Arterial dilation appears as increased ΔHbT contrast resulting from increased vessel volume and can be visualized as an increase in the physical diameter of the vessel (see also Figure 2g). Parenchymal hyperemia continues to rise slowly (iii); however,

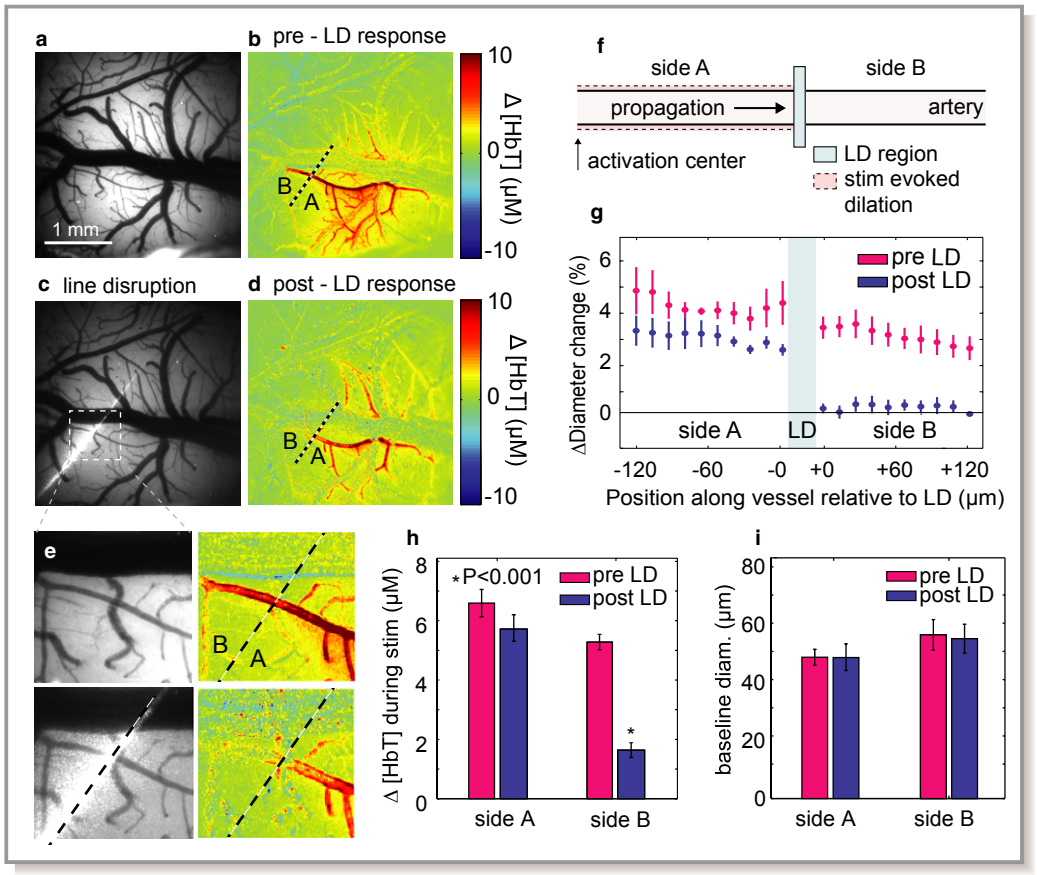

Figure 2. Light-line disruption to endothelial propagation of vasodilation. a, Grayscale image of the exposed cortical surface (534 nm-centered illumination). b, Pre-light-dye (LD) total hemoglobin (ΔHbT) functional response map (averaged over 4 to 6 seconds after stimulus onset, stimulus duration=12 seconds, average of N=5 runs from 1 rat). c, Image of 488 nm laser focused into a "light-line" positioned to transect a responding arteriole. d, Post-LD hemodynamic response equivalent to (b), average of N=5 runs from 1 rat. The dilatory response no longer reaches side B. e, Zoomed in views of the region indicated in (c) for each case shown in (a) through (d). f, Schematic showing LD treatment geometry. g, Percent change in vessel diameter at the response peak (4 to 6 seconds) relative to baseline on either side of the LD-treated vessel segment before (pink) and after (blue) LD treatment (average from n=3 rats, pre-LD runs=5 per rat, post-LD runs=5 per rat). Error bars: SEM. Position along the vessel is measured relative to the edges of the treated segment. The treated vessel segment was 83±15 μm long. h, Average ΔHbT 4 to 6 seconds after stimulus onset selected from side A and side B before (pink) and after (blue) LD treatment (n=4 rats, runs=20 per rat per condition). Side B shows significantly attenuated ΔHbT responses after LD treatment ($P<0.001$; Student t test). Error bars show SEs corrected for intraclass correlation. One rat included in ΔHbT analysis was excluded from diameter calculations owing to vessel overlap. i, Baseline vessel diameters on either side of the illuminated segment were unaffected by the LD treatment (n=3 rats, runs=15 per rat per condition: $P>0.7$, side A, $P>0.9$, side B; Student t test). Error bars show SEs corrected for intraclass correlation. Results from an additional light-line rat with acetylcholine (ACh) control are shown in Figure 4.

dilation in more-distant pial arteries begins to return to baseline after an initial peak at ~4 to 6 seconds (iv).[36,38] Continued stimulation maintains higher perfusion of a localized region of parenchyma in the center of the responding region, with minimal continued dilation of the more-distant pial arteries (v).[36,38–40] This difference is clear from ΔHbT time courses extracted from a "distant" pial artery versus the "center" of the responding region (Figure 1c). The "central" response exhibits an early peak and a later plateau phase,[36,38–40] whereas the "distant" component shows only an early peak. Models of neurovascular coupling to date have failed to explain these spatiotemporal patterns and have not presented a mechanism that can explain the long-range, rapid dilation of pial arteries both up- and downstream from the active region (see arterial flow vs. propagation directions indicated in Figure 1b). In earlier work, we characterized the onset propagation speed of this distant, retrograde pial artery dilation as exceeding 2 mm/s.[18] These observations led us to hypothesize that initial pial artery dilation involves rapidly propagated vasodilation within the vascular endothelium.[22]

Interruption of Retrograde Propagation of Vasodilation

To determine whether dilation of distant pial arteries is dependent on endothelial propagation of vasodilation, the light-dye method was implemented using a thin, focused line of 488 nm of laser light. This line was positioned and oriented to transect pial artery branches that had been observed to dilate in response to stimulation preceding light-dye treatment.

Figures 2a and 2b show a grayscale image of the exposed cortex and a corresponding ΔHbT functional map of the pre-light-dye cortical response to a 12-second hindpaw stimulus in 1 rat. A similar pattern of selective pial artery dilation can be seen as in Figure 1d. Figure 2c shows the location of the applied "light-line," intended to specifically disrupt endothelial signaling in a targeted pial artery. Figure 2d shows that following this light-line light-dye treatment, stimulus-evoked dilation of the artery segment distal to the light-dye treatment line (with respect to the center of the responding region) was strongly attenuated (side B). Arterial dilation on the proximal side (side A) was unaffected. Figure 2e shows a higher magnification view of the region indicated, for each case. This effect was consistent across all rats (n=4; $P<0.001$), both in terms of arterial diameter change (Figure 2g) and ΔHbT (Figure 2h).

It is important to note that the dilatory response was eradicated in the distal segment of vessel that was not itself illuminated by the light-dye laser, such that baseline diameters of each examined segment were the same before and after light-dye treatment (Figure 2i). Additional control measurements shown in Figure 4 confirm that dilation to application of ACh was observed on both sides of the light line. We conclude that selective, discrete disruption of the endothelium prevented transmission of stimulus-evoked vasodilatory signaling from the proximal (side A) to the distal segment (side B). We also note that this result clearly demonstrates that stimulus-evoked retrograde dilation of pial arteries is not the result of flow-mediated coupling.[41]

Wide-Field Disruption of the Vascular Endothelium

The light-line results described above provide strong evidence of an endothelial pathway for retrograde propagation of vasodilation along pial arteries during functional hyperemia. However, this result does not demonstrate the relative importance of this pathway in generating functional hyperemia as a whole. To address this, wide-field light-dye treatment was implemented using more distributed illumination from a LED centered at 470 nm. Because blue light is heavily scattered in brain tissue, we expect the main action of this illumination to be impairment of endothelial signaling within the superficial pial arteries (see Data S1 for depth analysis). The results from these measurements are summarized in Figure 3.

As expected, wide-field light-dye treatment significantly attenuated stimulus-evoked dilation of pial arteries (Figure 3a through 3d). Plotting the time courses of changes in ΔHbT occurring in the center of the responding region before and after light-dye treatment, we observe that wide-field light-dye disruption also has a strong effect on the overall ΔHbT time course (Figure 3e). Specifically, the fast increase and initial peak of the ΔHbT response is strongly attenuated, leaving behind only a gradual rise in Δ[HbT]. This residual response was found to localize to the parenchyma, rarely recruiting dilation of pial arteries. Equivalent results for a 2-second stimulus are compared in Figure S3. Corresponding HbO and HbR dynamics are shown in Figure S4.

Comparing these results to the spatiotemporal patterns shown in Figure 1, we note the similarity between the initial peak of the "distant" artery response in Figure 1c and the missing "peak" component of the ΔHbT response removed by wide-field light-dye treatment in Figure 3e. We also note the similarity between the spatial map of the pre-light-dye ΔHbT response at 14 to 16 seconds in Figure 1dv and the post-light-dye response (Figure 3d and 3e, same rat). This suggests that endothelium-dependent, long-range propagated vasodilation of pial arteries has a more significant role in the early phase and initial peak of the cortical hemodynamic response to stimulus than in later phases. We estimate that attenuation resulting from scattering and absorption in the intact brain would reduce the irradiance of wide-field 470 nm illumination to below the threshold for the light-dye effect within 100 to 200 microns of the pial surface (Data S1). This suggests that

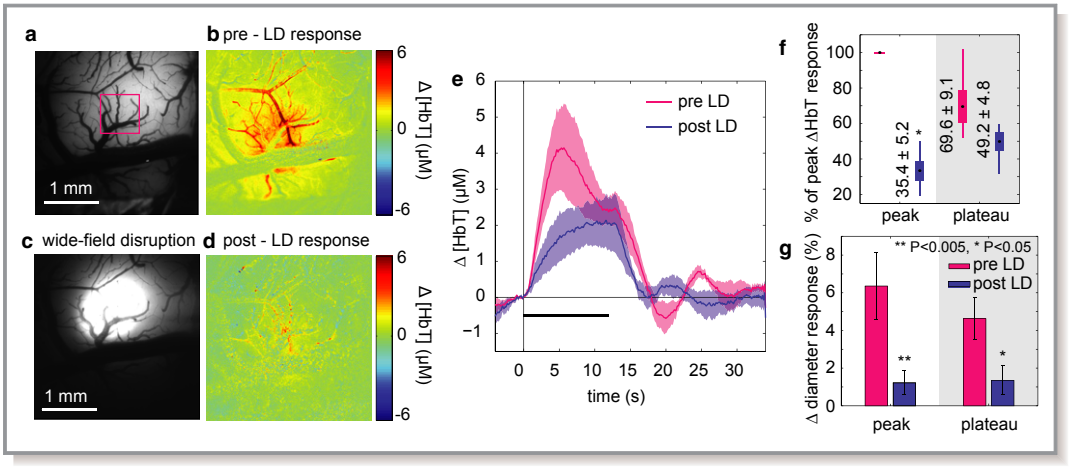

Figure 3. The hemodynamic response before and after wide-field light-dye treatment. a, grayscale image of the exposed cortical surface (534 nm-centered reflectance) of a representative rat (same rat as shown in Figure 1). b, Pre-light-dye treatment functional map showing total hemoglobin (Δ[HbT]) "peak" response relative to baseline averaged over 4 to 6 seconds after stimulus onset (average of N=5 runs, 1 rat). c, Image showing the blue light spot used for wide-field light-dye treatment (≈1 mm in diameter). d, Post-light-dye Δ [HbT] functional map (same rat, time-period average and color scale as [c]) (average of N=5 runs, 1 rat). e, Pre- and post-light-dye Δ[HbT] time-course response to 12 seconds of stimulation averaged over n=7 rats, runs=5 per rat per condition, responses averaged per rat. Error bounds show SEM over rats. Responses to 2-second stimulus are compared in Figure S3. Equivalent traces for oxy- and deoxy-hemoglobin concentration changes are shown in Figure S3. The region of interest was the same for all conditions and was centered over the responding region and included both arteries and parenchyma. f, Δ[HbT] amplitudes response averaged over the "peak" (4 to 6 seconds) and "plateau" (10 to 12 seconds) shown as a percentage of the pre-light-dye "peak" response (data from e). Black dots: mean, boxes: SEM, whiskers: range of data. Post-LD peak amplitude is significantly attenuated relative to pre-LD ($P<0.05$; Student *t* test). g, Percent stimulus-evoked change in diameter of responding pial arteries pre- and post-light-dye for "peak" and "plateau" (n=5 rats, 5 runs per rat per condition). Diameters calculated from averages of 5 runs=5 measurements per condition. Error bars show SEM. *P* values from Student *t* test.

our wide-field light-dye treatment most strongly affected the pial arteries, and therefore long-range signaling, leaving the endothelium of deeper segments of pial arterioles and capillaries intact.

Controls

To ensure that light-dye treatment was indeed *only* disrupting the vascular endothelium, and not smooth muscle cells, we performed established pharmacological control measurements at the end of each wide-field light-dye experiment.[22,24,33,42] Endothelium-dependent dilator ACh and endothelium-independent dilator SNP were each applied to the exposed cortex in turn, and MS-OISI data were acquired in the absence of stimulation. As expected, pial arteries in the untreated regions dilated to ACh application, whereas pial arteries within the treated area failed to dilate ($P<0.005$; Student *t* test), indicating endothelial disruption. The same treated arteries *did* dilate in response to SNP application, verifying that smooth muscle cells were intact and reactive after light-dye treatment (Figure 4a). Neither intravenous delivery of FITC-dx nor blue light exposure alone affected the amplitude of the peak response to stimulus or the baseline diameter of pial arteries (Figure 4b). ACh applied after light-line light-dye experiments caused *both* proximal and distal segments to dilate (Figure 4c through 4e), even though stimulus-evoked dilation of the same distal segment was significantly attenuated after light-line disruption. These results confirm that the distal segment was itself undamaged, and still physically able to dilate, indicating that the light line selectively interrupted the path taken by stimulus-evoked endothelial signaling. The data shown in Figure 4c through 4e were acquired in an animal under urethane anesthesia to rule out the influence of anesthesia on our findings. The slightly smaller pre-light-dye percentage stimulus-evoked arterial diameter increase seen here, compared to Figure 2, is likely a result of the larger baseline diameter of the chosen pial artery.

To assess whether wide-field light-dye treatment altered neuronal activity, microelectrode recordings of LFP were performed in 2 rats during 12 seconds of electrical hindpaw stimulation, before and after wide-field light-dye treatment. Traces in Figure 4f show identical patterns of larger amplitudes at stimulus onset, with a decay to lower amplitudes for the remainder of the stimulus. Individual LFPs also did not exhibit

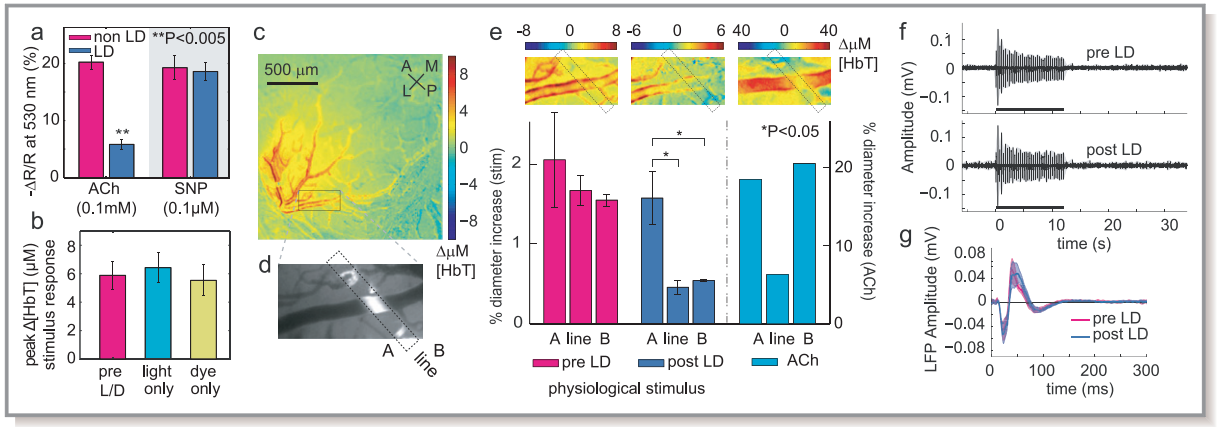

Figure 4. Smooth muscle cell function and neural activity were unaltered by light-dye treatment. a, Maximum Δ[HbT] change induced by topical cortical application of acetylcholine (ACh) (0.1 mmol/L) and sodium nitroprusside (SNP) (0.1 μmol/L) after wide-field light-dye (LD) treatment. LD values were extracted from within the treated blue light illumination area, whereas non-light-dye values were extracted from unilluminated, peripheral regions. Vasodilation to ACh in light-dye–treated regions was significantly attenuated (**P<0.005; Student t test; n=3 rats, 2 trials per rat per condition). The temporal dynamics of dilation to SNP in light-dye–treated and untreated regions were also unaffected (see Figure S6). b, Controls for 3 conditions: pre-light-dye response, response after exposure to blue light spot only (no dextran-conjugated fluorescein isothiocyanate (FITC-dx)), and response after FITC-dx dye intravenous injection only (no blue light). Peak Δ[HbT] response was averaged over the hindpaw response region between 4 and 6 seconds after stimulus onset (n=4 rats, average of 15 runs per rat for each condition, responses were averaged over 5 runs in each rat=12 measurements per condition; error bars show SEM) (P>0.6 and P>0.7, respectively; Student t test). c through f, Light-line ACh control. c, Peak Δ[HbT] map in response to 12-second stimulation averaged over 4 to 6 seconds after stimulus onset (d) shows the subregion during light-line illumination of a selected pial artery. e, Δ[HbT] images of same region of interest under 3 different conditions: (1) the peak response to stimulation before light-line treatment (N=5 runs); (2) the peak response to stimulation after light-line treatment (N=5 runs); and (3) The response of the same region (after light-line treatment) to topical application of ACh (1 trial). Bar graphs show calculated percentage change in diameter on either side of the light line for these 3 conditions in the same rat (stimulus results show an average of 10 repeated runs; error bars show SEM) *P<0.05; Student t test. f, Electrophysiological recordings of neural activity during 12 seconds of hindpaw stimulation before and after wide-field LD treatment. Black time course represents the average over n=2 rats, with runs=5 per rat per condition. Gray envelope indicates SEM. g, Averaged individual local field potential (LFP) spikes from the time courses in (f). Shaded region shows SEM.

significant differences in amplitude or shape throughout the stimulus period (Figure 4g), confirming that wide-field light-dye treatment did not itself alter neuronal activity.[38]

Our analysis of arterial diameters shown in Figure 3g did reveal one potential confound in our wide-field light-dye experiments: Pial arteries with baseline diameters between 30 and 50 μm exhibited a ≈19% (7.8±1.2 μm) increase in their baseline diameters after wide-field light-dye treatment. The predilating effect of light-dye treatment has been described previously[31,33,42] and does not imply that the vessel is unable to dilate further (as confirmed in every case by our SNP control). However, to verify that this predilation was not itself causing alterations to the hemodynamic response time course, we performed further in vivo control measurements in which we recorded responses to somatosensory stimulation during gradually increasing levels of predilation induced by a single topical application of 1 to 2 [micro]mol/L ACh (Data S5). Arteries that were predilated to equivalent levels, as induced by wide-field light-dye treatment, were found to still respond normally to somatosensory stimulation, with responses exhibiting a normal peak and plateau pattern and similar peak ΔHbT amplitudes as pre-light-dye response amplitudes, even for predilations exceeding 40%. This control demonstrates that moderate predilation alone does not affect the ability of pial arteries to dilate further in response to somatosensory stimulation. This result also shows that any increase in blood flow resulting from an increase in baseline diameters does not affect driving mechanisms sufficiently to alter the peak-plateau shape or amplitude of the response to stimulation.[38] We note also that our light-line results (Figures 2 and 4c through 4e) showed that discrete disruption of a small section of pial artery strongly attenuated dilation in distal arterial segments that were neither illuminated nor predilated. These distal segments were also responsive to ACh application, confirming that changes observed after light-dye treatment were not the result of physical damage to the unresponsive vessel segment. The small extent of the treated vessel segment in our light-line study also rules also out the possible influence of post-light-dye increases in baseline blood flow.

Additional analysis was performed to assess the possible influence of blood pressure and other systemic parameters. Our recordings of intra-arterial blood pressure indicated that a measurable decrease (up to 14%) in systemic blood pressure occurred in most rats immediately after FITC-dx injection. However, these changes in systemic blood pressure did not correlate with observed changes in arterial reactivity to stimulation, as evidenced by our "light-only" and "FITC-dx-only" measurements (Figure 4b). Similarly, whereas analysis also revealed a small (<2%) increase in systemic blood pressure in response to stimulation,[43] the temporal shape of these blood pressure responses were not significantly different for pre- and post-light-dye data. Light-line control experiments shown in Figure 4d and 4e were intentionally performed under intraperitoneal urethane anesthesia, rather than intravenous alphachloralose, to rule out the possible influence of anesthetic choice on our findings. In an equivalent cohort of animals, blood gases were found to be within normal ranges ($PaCO_2$ between 35 and 45 mm Hg, PaO_2 between 100 and 180 mm Hg, and pH between 7.3 and 7.45). In all cases, we conclude that the highly localized changes in the cortical patterns of stimulus-evoked arterial dilation that form the basis of our findings (Figure 2e) could not be the result of systemic effects.

Discussion

Our results provide strong evidence that the vascular endothelium is a critical pathway in functional neurovascular coupling. We showed that selective interruption of endothelial signaling blocked retrograde dilation of pial arteries in response to stimulus in the somatosensory cortex. Wide-field disruption of the vascular endothelium at the pial surface led to a significant attenuation of the hemodynamic response, particularly its initial peak.

These findings have important implications for earlier models of functional neurovascular coupling, as well as our understanding of the role that endothelial signaling might play in the brain.[7,8] Figure 5 illustrates known mechanisms for endothelial control of vasodilation alongside some of the brain-specific neurovascular coupling mechanisms proposed to date. The addition of the vascular endothelium to this picture appears to explain many of the anomalous findings in neurovascular coupling and fMRI research to date and raises a number of important new questions, as detailed below.

Which Types of Endothelial Mechanisms Might be Involved?

As illustrated in Figure 5, it is well established that in peripheral vasculature, stimulation of the vascular endothelium can initiate 2 types of propagated vasodilation: (1) endothelial hyperpolarization, which exhibits long-range and almost unattenuated propagation over distances exceeding a millimeter, and is insensitive to cyclooxygenase (COX) pathway and nitric oxide (NO) inhibitors,[20,22] and (2) a slower-moving (≈116 μm/s) calcium wave-associated propagated vasodilation that mediates vasodilation through endothelium-derived NO and prostanoids, such as prostacyclin (PGI_2), which decays over a distance of approximately 500 microns.[46] This "slow" mechanism has been shown to generate secondary vasodilation upon reaching arteriole segments already predilated by "fast" endothelial hyperpolarization, maintaining local dilation even after more-distant segments recover.[46] One study has suggested that higher levels of intracellular calcium release within the endothelium are required to generate endothelial hyperpolarization, compared to NO and prostanoid-dependent relaxation (340 vs. 220 nmol/L[47,48]).

The properties of these 2 "slow" and "fast" endothelial mechanisms fit well with the central/distant patterns of functional hyperemia shown in Figure 1, as well as the presence of residual parenchymal hyperemia after light-dye treatment (Figure 3e). We hypothesize that the initial, rapid, long-range dilation of pial arteries is consistent with long-range propagation of vasodilation by endothelial hyperpolarization. Consistent with this model, the more localized and sustained parenchymal hyperemia seen during prolonged stimulation could be dominated by slower and more spatially restricted NO and prostanoid-dependent mechanisms. This slower mechanism might more strongly influence diving arterioles and perhaps capillaries beyond the penetration depth of light-dye treatment (see Data S1).[46] Moreover, we note that endothelial hyperpolarization appears to be prominent at the onset of the response, short-lived, and largely independent of stimulus duration, whereas parenchymal hyperemia is sustained and more dependent on stimulus duration. We posit that this pattern may be representative of a thresholding effect, whereby endothelial hyperpolarization occurs only at the onset of stimulation, whereas slower NO and prostanoid-dependent dilation is repeatedly triggered by continuing stimulation.[47] This model appears to fit well with the nonlinearities routinely observed in fMRI blood-oxygen–level dependent (BOLD) data, as discussed further below.[49]

Can Endothelial Involvement Explain Previous Pharmacological Results?

To date, almost all attempts to pharmacologically impair functional hyperemia have observed some residual hyperemic response. In particular, studies seeking to block COX-1, COX-2, or NO pathways in order to isolate astrocyte and neuronal contributions, respectively, have found that neither

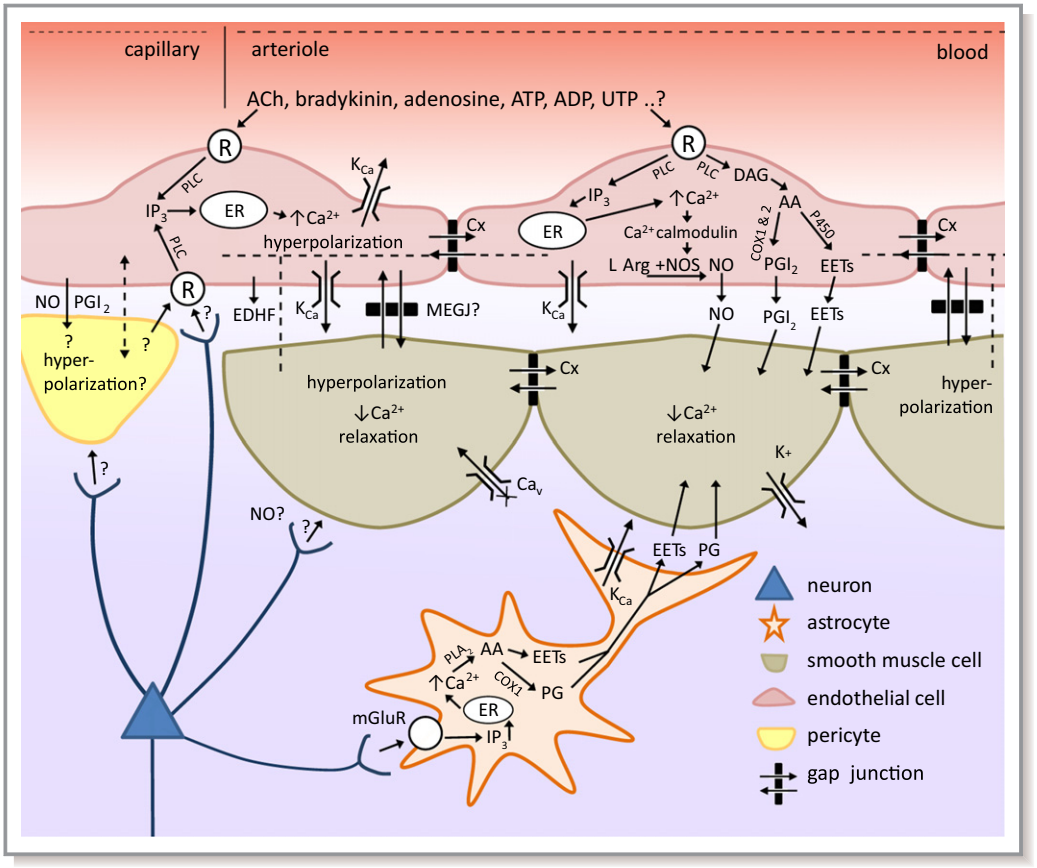

Figure 5. Incorporating the vascular endothelium into neurovascular coupling (adapted from refs. 44 and 7). Astrocyte: hypothesized to sense glutamate through metabotropic glutamate receptors (mGluR), increasing intracellular calcium $[Ca^{2+}]_{ia}$ and generating arachidonic acid (AA) from phospholipase A_2 (PLA_2) which is converted by COX1 (or 3) to prostaglandins (PG) and by P450 epoxygenase to epoxy-eicosatrienoic acid (EETs).[7,9] Both PGs and EETs can relax smooth muscle cells (SMCs). Endothelial cells can increase their intracellular calcium $[Ca^{2+}]_{ie}$ in response to receptor (R) binding (targets include acetylcholine (ACh), bradykinin (BK), adenosine triphosphate (ATP), adenosine diphosphate (ADP), uridine triphosphate (UTP), and adenosine[21,24–26]) causing inositol triphosphate (IP_3)-mediated release of calcium from the endothelial endoplasmic reticulum (ER).[19] Phospholipase C (or PLA_2), through diacyl-glycerol (DAG), can also produce EETs and AA derivatives, including prostacyclin (PGI_2) within endothelial cells, both of which can drive SMC relaxation whereas increased $[Ca^{2+}]_{ie}$ can also drive production of endothelial nitric oxide (NO), which can also relax SMCs. $[Ca^{2+}]_{ie}$ increases can also lead to endothelial hyperpolarization through opening of calcium-dependent potassium channels (K_{Ca}). Endothelial hyperpolarization can spread rapidly to adjacent endothelial cells through gap junctions and is coupled to encircling SMCs either through myoendothelial gap junctions (MEGJs) or some other "endothelium-derived hyperpolarizing factor" (EDHF).[19] SMC hyperpolarization causes relaxation through closure of voltage-dependent calcium channels (Ca_v). Signaling from excitatory and inhibitory cortical neurons[10,11] as well as afferents from regions such as the thalamus, basal forebrain, and locus coeruleus[4,45] to astrocytes, pericytes, SMCs have also been proposed.[2,7] Potential signaling pathways, yet identified, are indicated by question (?) marks, and include the possibility of signalling between astrocytes, pericytes and endothelial cells, or even direct neuronal signalling to the vascular endothelium at the capillary level.

(nor both) completely block functional hyperemia.[9,11,50] If both slow and fast endothelial pathways (as described above) are involved in functional hyperemia, then, as shown in Figure 5, components of stimulus-evoked vasodilation would be dependent on both endothelial-derived NO and prostanoids generated by endothelial COX pathways. Equally, endothelial hyperpolarization-mediated vasodilation, which is unaffected by COX and NO inhibition, would remain.[22] No previous neurovascular coupling studies have attributed a loss of attenuation of vasodilation under COX or NO inhibition to action on the vascular endothelium.[7] We propose that endothelial involvement in neurovascular coupling can explain many of the seemingly complex and paradoxical effects of these agents on functional neurovascular coupling, including

the presence of residual responses.[9,11] Studies relying on such pharmacological manipulations as evidence for the role of a particular cellular component in neurovascular coupling may have overlooked the possible action of these agents on the vascular endothelium.

Implications for Earlier Models of Neurovascular Coupling

Propagation of vasodilation within the vascular endothelium provides a mechanism to explain the retrograde selection and dilation of specific diving arterioles and pial artery branches. Studies proposing a role for astrocytes in functional neurovascular coupling have focused on interactions between astrocyte end-feet and the outer surface of perivascular smooth muscle cells on diving arterioles. However, recent studies challenging the role of astrocytes in neurovascular coupling have focused on discrepancies in the timing of measureable increases in intracellular calcium in astrocytes, which appear later than the onset of dilation in adjacent to diving arterioles.[17] Others have noted the lack of connectivity between astrocytes and reactive pial arteries above the glia limitans.[17,27,51] We propose that propagated vasodilation might explain these discrepancies by removing the requirement for astrocyte control of blood flow at the level of diving arterioles.[15,17] We note that the generally slow intracellular calcium responses observed in astrocytes may implicate astrocyte involvement in the later phases of functional hyperemia.[15,40,52] However, we also note that a recent study suggesting that more-rapid astrocyte responses may be present around capillaries[12] might imply a direct relationship with the vascular endothelium at the capillary level.

Additional recent studies that have begun to explore the role of pericytes in the active modulation of capillary tone.[6,13,53] Pericytes have been shown in vitro to relax *in response* to PGI_2, NO, and bradykinin,[6] making them an intriguing partner for ECs, either to assist in initiation of propagated vasodilation or to receive signals *from* ECs in a similar way to arterial smooth muscle cells (Figure 5).

How Might Endothelial Signaling be Initiated in the Brain?

The involvement of endothelial signaling in functional neurovascular coupling implies that this signaling must, at some point, be initiated. In the peripheral vasculature, endothelial hyperpolarization can be initiated through activation of endothelial G-protein-coupled receptors sensitive to signaling molecules and neurotransmitters, including ACh, adenosine, adenosine triphosphate (ATP), adenosine diphosphate (ADP), uridine triphosphate, K^+ ions, and bradykinin.[8,21,24–26] Although innervation of the microvasculature by ACh-expressing afferents has been explored,[54,55] many other pathways might be viable candidates for initiation of endothelially driven vasodilation and could feasibly involve direct neuronal signaling to the endothelium or signaling through intermediaries, such as astrocytes, pericytes, or smooth muscle cells.[7,9,11–13,40] These potentially neurogenic mechanisms for the initiation of functional hyperemia have not been explored to date.

Endothelial propagation also obviates the need for some extravascular network to dictate *which* penetrating arterioles should be chosen to dilate in order to increase capillary flow at a given site of initiation.[10,17,18] The endothelium provides an integrative conduit for signaling, which would be expected to find the shortest route to larger arteries, selecting the optimal arteriolar branches to generate a localized increase in blood flow.[56] ATP-evoked endothelial propagation of vasodilation has been shown to be able to fully traverse the capillary bed from its venous to arterial side in a hamster cheek pouch model.[57] Our results therefore suggest that initiators and mediators of neurovascular coupling could be located at the capillary bed and do not necessarily need to contact the abluminal surface of penetrating arteriole smooth muscle cells.[57] Initiation at the capillary bed would also be consistent with signaling originating at the location of highest metabolic demand.

Implications for Interpretation of fMRI Studies

A primary concern in the analysis and interpretation of fMRI data is whether observed responses can be inferred to directly represent neuronal activity.[2] Numerous studies have noted nonlinearities in the spatiotemporal properties of the fMRI response showing, for example, invariance in response amplitude and temporal shape for stimuli ranging between 5 ms and 2 seconds.[39,49] Several previous studies of the nonlinear properties of the fMRI response have led some to explore and model the possibility of a 2-component (or more) mechanism for neurovascular coupling, although without an explicit mechanistic basis.[38–40,49,58]

Although more work is needed to carefully characterize the properties and dynamics of endothelium-driven vasodilation in the brain, we propose that many aspects of the BOLD response might be explained through consideration of the spatiotemporal and, possibly, threshold-dependent properties of endothelial signaling, both fast and slow.[20,22,46] Uncovering the mechanisms initiating endothelial hyperpolarization during functional hyperemia would provide critical insight into whether responses to short (or long) duration stimuli, or to spontaneous activity in resting state fMRI, can indeed be interpreted as directly neurogenic.[2] The specific properties of

endothelium-dependent mechanisms could also provide a basis for the finest achievable "functional" spatial resolution of fMRI.[59,60]

Synergy Between Vascular Control in the Brain and Body

Our findings suggest a closer relationship than previously considered between functional hemodynamic regulation in the brain and the rest of the body. Consistent with our findings, we note that spatiotemporal properties of endothelial hyperpolarization in peripheral vasculature closely match the behavior of pial arteries during functional hyperemia, including the speed and range of initial retrograde vasodilation, and the timing of the peak and return to baseline after short stimuli.[8,18–20,22,23,25] Studies of blood flow control in skeletal muscle have already introduced the idea of an integrative vascular signaling pathway that fine-tunes local perfusion through retrograde vasodilation from capillaries (in areas of demand) to larger arterioles.[18,60–62]

The primary studies providing evidence *against* endothelial propagation of vasodilation in neurovascular coupling have proposed that signaling from the glia limitans might mediate stimulus-evoked dilation of pial arteries.[27,63] In Xu et al. 24-hour exposure to the gliotoxin, L-α-aminoadipic acid, was found to eradicate in vivo pial arterial dilations in vivo in response to bicuculine suffusion and sciatic nerve stimulation, whereas light-dye treatment failed to significantly attenuate the same dilations. The major difference between this and our study is the intensity and duration of the stimulation used. Bicuculine suffusion induced seizure-level neuronal firing and arterial dilations of over 30% of baseline diameters over the course of up to 20 minutes (compared to approximately 6% dilations for <16 seconds in our study). The strong, direct sciatic nerve stimulation used by Xu et al. lasted for 20 seconds, but induced massive arterial dilations exceeding 35% of baseline diameters, peaking around 40 seconds after stimulus onset. Similarly, Kanu et al., who studied the influence of L-α-aminoadipic acid on pial artery dilation in newborn piglets, used direct cortical application of ADP in order to induce ≈30% increases in pial artery diameter over the course of 3 minutes.[63] We conclude that pial arterial dilations induced by stronger, more prolonged stimuli may be governed by a different mechanism than responses to the more physiological levels of native stimulus presented in our experiments. Other studies have explored the presence of specific connexins on cerebral vessels as evidence for endothelial involvement. Kao et al.[28] examined vessels in the brainstem and found little evidence of connexin 40 and 37 in the microvasculature, but noted strong expression in brainstem pial arteries and larger penetrating arterioles. However, cortical vessels were not studied, and it should be noted that questions remain regarding the specific gap junction components involved in endothelial propagation of vasodilation.[20,32,48] Moreover, numerous studies have independently verified the ability of cerebral vessels to conduct vasodilation within their endothelium.[8,23–26]

Implications for Brain Health

Stimulus-evoked cortical hyperemia serves to tune local blood flow levels to the demands of active neurons. This dynamic modulation of blood flow may be as critical to maintaining normal brain function as baseline flow levels.

Impairment of neurovascular coupling has been implicated in Alzheimer's disease and neurodegeneration.[4–6] However, a wider range of systemic pathologies are known to involve the dysfunction of the vascular endothelium, including cardiovascular disease and diabetes, many of which have associated neural deficits that go beyond simple factors, such as cardiac output.[64] A number of studies have noted alterations in fMRI BOLD responses, and therefore possible neurovascular dysfunction, in aging,[3] diabetes,[65] hypertension,[66] and microangiopathy.[67] Exploration of a link between neurovascular dysfunction and cognitive decline could provide new avenues for the development of diagnostic tools and therapeutic interventions.

We also note that the vascular endothelium is directly exposed to the bloodstream, suggesting that even drugs that do not cross the blood–brain barrier, but act on the endothelium, could influence neurovascular coupling.[3,9] One study demonstrated that intravenous indomethacin and rofecoxib (a nonsteroidal anti-inflammatory) both cause attenuation of the cortical hemodynamic response to somatosensory stimulation.[68] The data shown are consistent with a reduction in the later slow phase of functional hyperemia, suggesting impairment of prostanoid/NO signaling, consistent with our 2-phase model. The possible involvement of multiple endothelial pathways, dependent on COX-1, COX-2, NO, and, perhaps, ACh or bradykinin, significantly increases the number of anti-inflammatory, analgesic, antihypertensive, and other drugs that could potentially influence functional neurovascular coupling. Involvement of the endothelium in neurovascular coupling provides a mechanistic basis for drug-induced alterations to the fMRI response, but also highlights the potential for systemic drugs to have either positive or negative influences on brain health through alteration or enhancement of neurovascular coupling.

In summary, our results demonstrate that an intact vascular endothelium is critical for the generation of a full hemodynamic response to stimulus in the brain. This result provides a new roadmap for understanding neurovascular coupling as well as for interpreting functional imaging signals. Our findings also highlight the arterial endothelium as a possible component to be explored in relation to brain

pathologies, such as neurodegeneration, as well as a potentially accessible therapeutic target.

Acknowledgments

The authors thank Profs Caryl Hill and Costantino Iadecola for their guidance and helpful discussions and Sasha Rayshubskiy and Timothy Muldoon for their intellectual contributions and assistance with experimental techniques.

Sources of Funding

The authors acknowledge support from National Institutes of Health grants: R01 NS063226, R01 NS076628, and R21 NS053684 (Hillman) and F31 NS084538 (Kozberg), National Institute for Neurological Disorders and Stroke (NINDS), R01 EY019500 (Das), National Eye Institute (NEI), T32 GM007367 MSTP (Shelanski), National Institute of General Medical Sciences (NIGMS), UL1 TR000040 (Ginsburg), National Center for Advancing Translational Sciences (NCATS), National Science Foundation grants: CAREER 0954796 (Hillman), graduate fellowships (Chen, Bouchard), National Defense Science and Engineering Graduate fellowship (Bouchard), the Human Frontier Science Program, the Kavli Foundation and the Rodriguez family.

Disclosures

None.

References

1. Sirotin YB, Hillman EMC, Bordier C, Das A. Spatiotemporal precision and hemodynamic mechanism of optical point spreads in alert primates. *Proc Natl Acad Sci USA*. 2009;106:18390–18395.
2. Attwell D, Iadecola C. The neural basis of functional brain imaging signals. *Trends Neurosci*. 2002;25:621–625.
3. D'Esposito M, Deouell LY, Gazzaley A. Alterations in the BOLD fMRI signal with ageing and disease: a challenge for neuroimaging. *Nat Rev Neurosci*. 2003;4:863–872.
4. Girouard H, Iadecola C. Neurovascular coupling in the normal brain and in hypertension, stroke, and Alzheimer disease. *J Appl Physiol*. 2006;100:328–335.
5. Iadecola C. The pathobiology of vascular dementia. *Neuron*. 2013;80:844–866.
6. Hamilton NB, Attwell D, Hall CN. Pericyte-mediated regulation of capillary diameter: a component of neurovascular coupling in health and disease. *Fron Neuroenergetics*. 2010;2:pii:5
7. Attwell D, Buchan AM, Charpak S, Lauritzen M, MacVicar BA, Newman EA. Glial and neuronal control of brain blood flow. *Nature*. 2010;468:232–243.
8. Andresen J, Shafi NI, Bryan RM. Endothelial influences on cerebrovascular tone. *J Appl Physiol*. 2006;100:318–327.
9. Takano T, Tian G, Peng W, Lou N, Libionka W, Han X, Nedergaard M. Astrocyte-mediated control of cerebral blood flow. *Nat Neurosci*. 2006;9:260–267.
10. Cauli B, Tong X-K, Rancillac A, Serluca N, Lambolez B, Rossier J, Hamel E. Cortical GABA interneurons in neurovascular coupling: relays for subcortical vasoactive pathways. *J Neurosci*. 2004;24:8940–8949.
11. Lecrux C, Toussay X, Kocharyan A, Fernandes P, Neupane S, Lévesque M, Plaisier F, Shmuel A, Cauli B, Hamel E. Pyramidal neurons are "neurogenic hubs" in the neurovascular coupling response to Whisker stimulation. *J Neurosci*. 2011;31:9836–9847.
12. Lind BL, Brazhe AR, Jessen SB, Tan FCC, Lauritzen MJ. Rapid stimulus-evoked astrocyte Ca^{2+} elevations and hemodynamic responses in mouse somatosensory cortex in vivo. *Proc Natl Acad Sci USA*. 2013;110:E4678–E4687.
13. Fernández-Klett F, Offenhauser N, Dirnagl U, Priller J, Lindauer U. Pericytes in capillaries are contractile in vivo, but arterioles mediate functional hyperemia in the mouse brain. *Proc Natl Acad Sci USA*. 2010;107:22290–22295.
14. Sun W, McConnell E, Pare J-F, Xu Q, Chen M, Peng W, Lovatt D, Han X, Smith Y, Nedergaard M. Glutamate-dependent neuroglial calcium signaling differs between young and adult brain. *Science*. 2013;339:197–200.
15. Nizar K, Uhlirova H, Tian P, Saisan PA, Cheng Q, Reznichenko L, Weldy KL, Steed TC, Sridhar VB, MacDonald CL, Cui J, Gratiy SL, Sakadžić S, Boas DA, Beka TI, Einevoll GT, Chen J, Masliah E, Dale AM, Silva GA, Devor A. In vivo stimulus-induced vasodilation occurs without IP3 receptor activation and may precede astrocytic calcium increase. *J Neurosci*. 2013;33:8411–8422.
16. Takata N, Nagai T, Ozawa K, Oe Y, Mikoshiba K, Hirase H. Cerebral blood flow modulation by basal forebrain or Whisker stimulation can occur independently of large cytosolic Ca^{2+} signaling in astrocytes. *PLoS One*. 2013;8:e66525.
17. McCaslin AFH, Chen BR, Radosevich AJ, Cauli B, Hillman EMC. In-vivo 3D morphology of astrocyte-vasculature interactions in the somatosensory cortex: implications for neurovascular coupling. *J Cereb Blood Flow Metab*. 2011;31:795–806.
18. Chen BR, Bouchard MB, McCaslin AFH, Burgess SA, Hillman EMC. High-speed vascular dynamics of the hemodynamic response. *Neuroimage*. 2011;54:1021–1030.
19. Bagher P, Segal SS. Regulation of blood flow in the microcirculation: role of conducted vasodilation. *Acta Physiol*. 2011;202:271–284.
20. Figueroa XF, Duling BR. Dissection of two Cx37-independent conducted vasodilator mechanisms by deletion of Cx40: electrotonic versus regenerative conduction. *Am J Physiol Heart Circ Physiol*. 2008;295:H2001–H2007.
21. Winter P, Dora KA. Spreading dilatation to luminal perfusion of ATP and UTP in rat isolated small mesenteric arteries. *J Physiol*. 2007;582:335–347.
22. Wölfle SE, Chaston DJ, Goto K, Sandow SL, Edwards FR, Hill CE. Non-linear relationship between hyperpolarisation and relaxation enables long distance propagation of vasodilatation. *J Physiol*. 2011;589:2607–2623.
23. Hannah RM, Dunn KM, Bonev AD, Nelson MT. Endothelial SKCa and IKCa channels regulate brain parenchymal arteriolar diameter and cortical cerebral blood flow. *J Cereb Blood Flow Metab*. 2011;31:1175–1186.
24. Rosenblum WI. Endothelial dependent relaxation demonstrated in vivo in cerebral arterioles. *Stroke*. 1986;17:494–497.
25. Marrelli SP, Eckmann MS, Hunte MS. Role of endothelial intermediate conductance KCa channels in cerebral EDHF-mediated dilations. *Am J Physiol Heart Circ Physiol*. 2003;285:H1590–H1599.
26. You J, Johnson TD, Childres WF, Bryan RM. Endothelial-mediated dilations of rat middle cerebral arteries by ATP and ADP. *Am J Physiol Heart Circ Physiol*. 1997;273:H1472–H1477.
27. Xu H-L, Mao L, Ye S, Paisansathan C, Vetri F, Pelligrino DA. Astrocytes are a key conduit for upstream signaling of vasodilation during cerebral cortical neuronal activation in vivo. *Am J Physiol Heart Circ Physiol*. 2008;294:H622–H632.
28. Kuo IY, Chan-Ling T, Wojcikiewicz RJ, Hill CE. Limited intravascular coupling in the rodent brainstem and retina supports a role for glia in regional blood flow. *J Comp Neurol*. 2008;511:773–787.
29. Gordon GRJ, Mulligan SJ, MacVicar BA. Astrocyte control of the cerebrovasculature. *Glia*. 2007;55:1214–1221.
30. Bouchard MB, Chen BR, Burgess SA, Hillman EMC. Ultra-fast multispectral optical imaging of cortical oxygenation, blood flow, and intracellular calcium dynamics. *Opt Express*. 2009;17:15670–15678.
31. Emerson GG, Segal SS. Endothelial cell pathway for conduction of hyperpolarization and vasodilation along hamster feed artery. *Circ Res*. 2000;86:94–100.
32. Howitt L, Chaston DJ, Sandow SL, Matthaei KI, Edwards FR, Hill CE. Spreading vasodilatation in the murine microcirculation: attenuation by oxidative stress-induced change in electromechanical coupling. *J Physiol*. 2013;591:2157–2173.
33. Bartlett IS, Segal SS. Resolution of smooth muscle and endothelial pathways for conduction along hamster cheek pouch arterioles. *Am J Physiol Heart Circ Physiol*. 2000;278:H604–H612.
34. Tian P, Devor A, Sakadžić S, Dale AM, Boas DA. Monte Carlo simulation of the spatial resolution and depth sensitivity of two-dimensional optical imaging of the brain. *J Biomed Opt*. 2011;16:016006–016006-016013
35. Hillman EMC. Optical brain imaging in-vivo: techniques and applications from animal to man. *J Biomed Opt*. 2007;12:051402.

36. Berwick J, Johnston D, Jones M, Martindale J, Martin C, Kennerley AJ, Redgrave P, Mayhew JEW. Fine detail of neurovascular coupling revealed by spatiotemporal analysis of the hemodynamic response to single whisker stimulation in rat barrel cortex. *J Neurophysiol*. 2008;99:787–798.
37. Tian P, Teng IC, May LD, Kurz R, Lu K, Scadeng M, Hillman EM, De Crespigny AJ, D'Arceuil HE, Mandeville JB, Marota JJ, Rosen BR, Liu TT, Boas DA, Buxton RB, Dale AM, Devor A. Cortical depth-specific microvascular dilation underlies laminar differences in blood oxygenation level-dependent functional MRI signal. *Proc Natl Acad Sci USA*. 2010;107:15246–15251.
38. Kennerley AJ, Harris S, Bruyns-Haylett M, Boorman L, Zheng Y, Jones M, Berwick J. Early and late stimulus-evoked cortical hemodynamic responses provide insight into the neurogenic nature of neurovascular coupling. *J Cereb Blood Flow Metab*. 2012;32:468–480.
39. Martindale J, Berwick J, Martin C, Kong Y, Zheng Y, Mayhew J. Long duration stimuli and nonlinearities in the neural-haemodynamic coupling. *J Cereb Blood Flow Metab*. 2005;25:651–661.
40. Cauli B, Hamel E. Revisiting the role of neurons in neurovascular coupling. *Fron Neuroenergetics*. 2010;2:9.
41. Ngai AC, Winn HR. Modulation of cerebral arteriolar diameter by intraluminal flow and pressure. *Circ Res*. 1995;77:832–840.
42. Leffler CW, Mirro R, Shanklin DR, Armstead WM, Shibata M. Light/dye microvascular injury selectively eliminates hypercapnia-induced pial arteriolar dilation in newborn pigs. *Am J Physiol Heart Circ Physiol*. 1994;266:H623–H630.
43. Kozberg MG, Chen BR, DeLeo SE, Bouchard MB, Hillman EMC. Resolving the transition from negative to positive blood oxygen level-dependent responses in the developing brain. *Proc Natl Acad Sci USA*. 2013;110:4380–4385.
44. Félétou M, Vanhoutte PM. EDHF: new therapeutic targets? *Pharmacol Res*. 2004;49:565–580.
45. Bekar LK, Wei HS, Nedergaard M. The locus coeruleus-norepinephrine network optimizes coupling of cerebral blood volume with oxygen demand. *J Cereb Blood Flow Metab*. 2012;32:2135–2145.
46. Tallini YN, Brekke JF, Shui B, Doran R, Hwang SM, Nakai J, Salama G, Segal SS, Kotlikoff MI. Propagated endothelial Ca^{2+} waves and arteriolar dilation in vivo: measurements in Cx40BAC–GCaMP2 transgenic mice. *Circ Res*. 2007;101:1300–1309
47. Marrelli SP. Mechanisms of endothelial P2Y1- and P2Y2-mediated vasodilatation involve differential $[Ca^{2+}]$i responses. *Am J Physiol Heart Circ Physiol*. 2001;281:H1759–H1766.
48. de Wit C, Griffith T. Connexins and gap junctions in the EDHF phenomenon and conducted vasomotor responses. *Pflugers Arch*. 2010;459:897–914.
49. Yeşilyurt B, Uğurbil K, Uludağ K. Dynamics and nonlinearities of the BOLD response at very short stimulus durations. *Magn Reson Imaging*. 2008;26:853–862.
50. Lindauer U, Megow D, Matsuda H, Dirnagl U. Nitric oxide: a modulator, but not a mediator, of neurovascular coupling in rat somatosensory cortex. *Am J Physiol*. 1999;277:H799–H811.
51. Iadecola C, Nedergaard M. Glial regulation of the cerebral microvasculature. *Nat Neurosci*. 2007;10:1369–1376.
52. Wang X, Lou N, Xu Q, Tian G, Peng WG, Han X, Kang J, Takano T, Nedergaard M. Astrocytic Ca^{2+} signaling evoked by sensory stimulation in vivo. *Nat Neurosci*. 2006;9:816–823.
53. Hall CN, Reynell C, Gesslein B, Hamilton NB, Mishra A, Sutherland BA, O'Farrell FM, Buchan AM, Lauritzen M, Attwell D. Capillary pericytes regulate cerebral blood flow in health and disease. *Nature*. 2014;508:55–60.
54. Hamel E. Cholinergic Modulation of the Cortical Microvascular Bed. In: Laurent Descarries KK, Mircea S, eds. *Progress in Brain Research*. Amsterdam, Netherlands: Elsevier; 2004:171–178.
55. Sato A, Sato Y. Cholinergic neural regulation of regional cerebral blood flow. *Alzheimer Dis Assoc Disord*. 1995;9:28–38.
56. Duza T, Sarelius IH. Conducted dilations initiated by purines in arterioles are endothelium dependent and require endothelial Ca^{2+}. *Am J Physiol Heart Circ Physiol*. 2003;285:H26–H37.
57. Collins DM, McCullough WT, Ellsworth ML. Conducted vascular responses: communication across the capillary bed. *Microvasc Res*. 1998;56:43–53.
58. Tomita M. Blood flow control in the brain: possible biphasic mechanism of functional hyperemia. *Asian Biomed*. 2007;1:17–32.
59. Harrison RV, Harel N, Panesar J, Mount RJ. Blood capillary distribution correlates with hemodynamic based functional imaging in cerebral cortex. *Cereb Cortex*. 2002;12:225–233.
60. Tran CHT, Vigmond EJ, Goldman D, Plane F, Welsh DG. Electrical communication in branching arterial networks. *Am J Physiol Heart Circ Physiol*. 2012;303:H680–H692.
61. Sarelius I, Pohl U. Control of muscle blood flow during exercise: local factors and integrative mechanisms. *Acta Physiol*. 2010;199:349–365.
62. Erinjeri JP, Woolsey TA. Spatial integration of vascular changes with neural activity in mouse cortex. *J Cereb Blood Flow Metab*. 2002;22:353–360.
63. Kanu A, Leffler CW. Roles of glia limitans astrocytes and carbon monoxide in adenosine diphosphate-induced pial arteriolar dilation in newborn pigs. *Stroke*. 2009;40:930–935.
64. Jefferson AL. Cardiac output as a potential risk factor for abnormal brain aging. *J Alzheimers Dis*. 2010;20:813–821.
65. Mogi M, Horiuchi M. Neurovascular coupling in cognitive impairment associated with diabetes mellitus. *Circ J*. 2011;75:1042–1048.
66. Jennings JR, Muldoon MF, Ryan C, Price JC, Greer P, Sutton-Tyrrell K, van der Veen FM, Meltzer CC. Reduced cerebral blood flow response and compensation among patients with untreated hypertension. *Neurology*. 2005;64:1358–1365.
67. Schroeter ML, Cutini S, Wahl MM, Scheid R, Yves von Cramon D. Neurovascular coupling is impaired in cerebral microangiopathy—An event-related Stroop study. *NeuroImage*. 2007;34:26–34.
68. Bakalova R, Matsuura T, Kanno I. The cyclooxygenase inhibitors indomethacin and Rofecoxib reduce regional cerebral blood flow evoked by somatosensory stimulation in rats. *Exp Biol Med*. 2002;227:465–473.

Supplemental figures and supporting information

Contents

S1. Light-dye illumination penetration analysis

The blue light illumination used for light-dye treatment in our studies will be both scattered and absorbed within brain tissue. The light-dye effect depends on three parameters; the concentration of FITC within the vessel, the irradiance (mW / mm^2) of illumination and the duration of the exposure. The values chosen in our experiments were based on literature review and preliminary studies that assessed irradiance and duration of illumination that was adequate to result in disruption of endothelial signaling in pial arteries, while leaving smooth muscle function intact (and producing no measurable damage in other vessels). The values chosen were 5-6 minutes of exposure with irradiance of 488 or 473 nm light at the cortex of ~6 mW/mm^2. However, it is important for us to consider whether this illumination at the surface may have also affected vessels deeper within the cortex.

Fortunately, much attention in recent years has been paid to the propagation of blue light within the rodent cortex, since the light used for light-dye experiments is identical to that used in optogenetics studies [2]. In optogenetics, it is important to assess how far blue light penetrates into the brain before being attenuated to a point where it no longer meets the threshold for optogenetic excitation. In our case, these prior measurements and modeled values can provide insight into the action of light-dye.

Most measurements of blue light propagation in brain tissue have been performed in ex-vivo brain tissues [3]. This will likely over-estimate penetration of light, since in-vivo propagation of blue light will be strongly influenced by hemoglobin in this range. In our case, FITC is also present, which strongly absorbs at 473 and 488 nm. Optogenetic simulation geometries also generally assume a fiber optic illumination with specified fiber diameter, numerical aperture and distance between the fiber and brain. However, our illumination geometry can be readily modeled in these terms, with our 'wide-field' illumination being equivalent to a ~1,000 micron diameter fiber with low NA (e.g. 0.01) in contact with the brain's surface, while our 'light-line' illumination (along its focused axis) would be equivalent to a 0.025 NA fiber with a 50 micron diameter also in contact with the tissue.

A model based on Kubelka-Munk theory (ignoring contributions from absorption) predicts Figure S1, which shows the intracortical irradiance for each of these geometries (assuming S = 10.3 mm^{-1} for rat brain, measured in [3]).

This very conservative estimate (since this model is based on brain slice measurements with no absorbing blood or FITC present) suggests that the irradiance reduces to 50% at a depth of around 100 microns, and to around 10% at a depth of 400 microns. Our light-line geometry is slightly more superficially weighted. These estimates are consistent with a number of other studies using empirical measurements and Monte Carlo simulations [4,5].

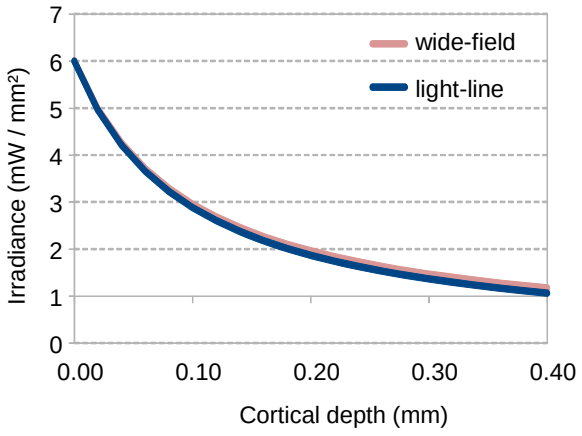

Figure S1. Calculated intensity of 488 nm blue light in the rat cortex as a function of depth for our two different light-dye geometries.

While quantification of the exact irradiance threshold for light-dye treatment is difficult to discern, we certainly noted in our original experiments that reducing either illumination or duration of exposure by half failed to achieve the endothelium-disruption effect of light-dye treatment. We therefore estimate that the action of

our light-dye experiments was constrained to vasculature within the top 100-200 microns of the cortex. As illustrated in figure S2 below, this depth will mostly affect pial arteries and the top segments of diving arterioles, but deeper arterioles likely maintain their function.

S2. Depth sensitivity and interpretation of MS-OISI

Similar analysis to that presented above can also be used to understand the meaning and origin of cortical signals observed using MS-OISI. A recent, detailed paper by Tian et al directly addressed this issue using Monte Carlo simulations of the sensitivity of visible light to cortical changes in absorption [1]. It should be noted that the level of light penetration (shown above) is not the same as a sensitivity measure, since the light detected by a camera must travel back out of the tissue before being detected. Parameters such as the lateral size of the responding region and the numerical aperture of the detection optics therefore also play a role in governing depth sensitivity. However, analyzing these variables, Tian et al showed that at 633 nm, absorption changes occurring at a depth between 200-300 microns contribute around 15% to the total detected signal, compared to ~32% for equivalent changes occurring in the top 100 microns, and ~5% from changes originating at depths between 300-400 microns (~ layer III). The study also demonstrates the 'blurring' effect of depth, such that a small, laterally discrete region at a depth of 400 microns would have a spatial resolution of 100-300 microns. In practice, this explains why individual capillaries or other sub-pial vessels cannot be spatially resolved, however, they do contribute substantially to the MS-OISI signals detected at the superficial cortex. Since superficial vessels are only very minimally blurred, and since the structure of the cortical vasculature is laid out to have all of the horizontally traveling pial vessels at the surface, this capillary / diving vessel signal can be discerned from signal changes seen in-between pial vessels. This is illustrated schematically in figure S2 below.

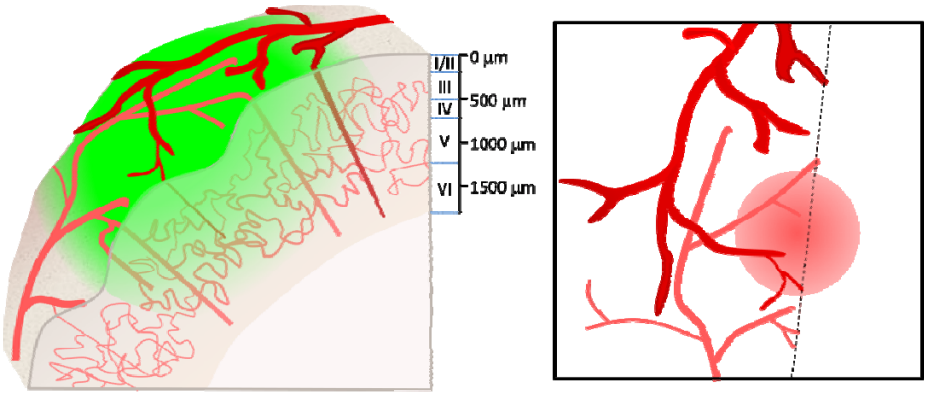

Figure S2. The spatial sensitivity and resolution of MS-OISI. Left: 3D schematic of the rodent cortex showing surface illumination with green light. The cross-sectional vascular organization of the cortex means that most large vessels are located on the pial surface, with diving arterioles and venules feeding deeper capillary beds. Right: sketch of the same section of cortex viewed en-face by MS-OISI (dotted line illustrates cut-through section shown left). Surface vessels appear strong and sharp. Contributions from changes in deeper capillary beds and diving vessels contribute to the more diffuse background signal seen in the 'parenchyma'.

S3. Comparison of 12 and 2 second stimulus duration pre/post light-dye

The pre- and post-LD response for 2 second stimulation show identical time-courses to the 12 second stimulation up to t = 2 seconds. After cessation of the 2 second stimulus, the post-LD response begins to return to baseline slightly before the pre-LD response. Considering the response magnitude as the area under each curve, wide-field light-dye treatment targeting pial arteries appears to have a larger net effect on the hemodynamic response to shorter stimuli. This is consistent with endothelial hyperpolarization dominating the early phase of the response.

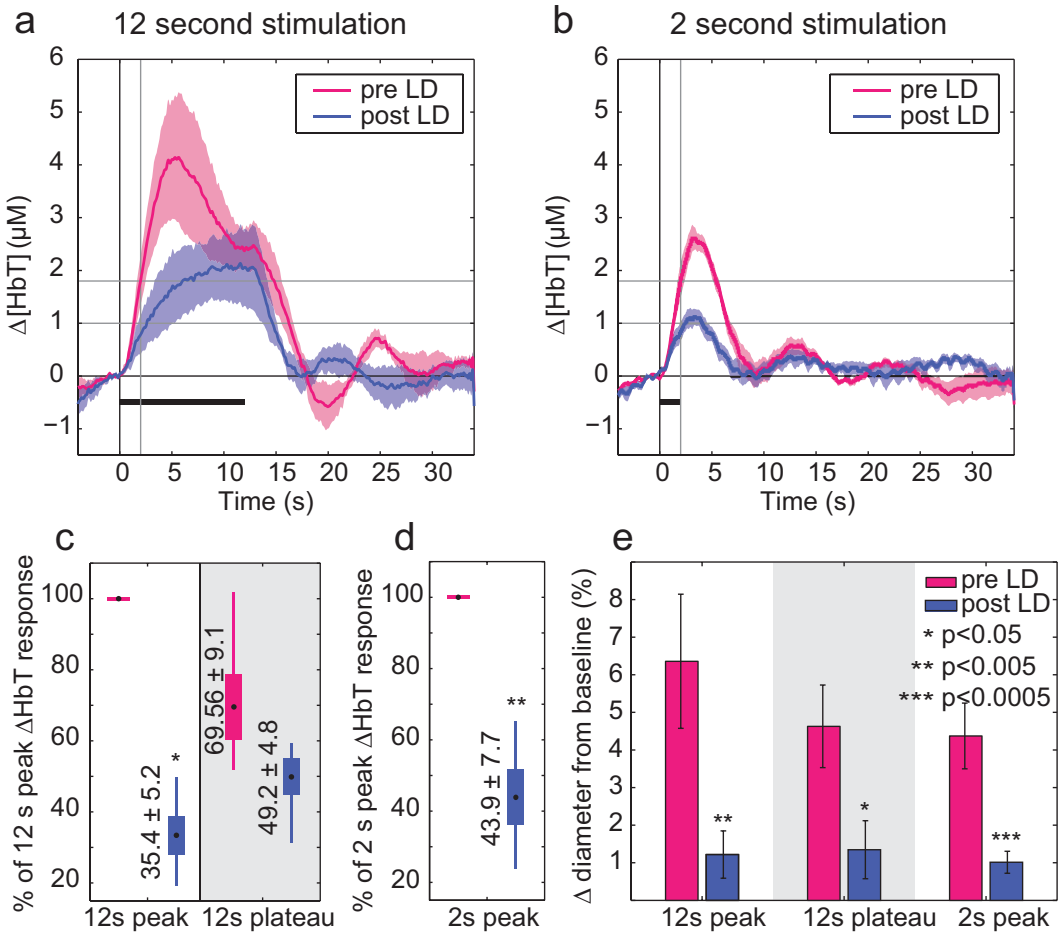

Figure S3. Comparison of the effect of wide-field light-dye treatment for 12 and 2 second stimulus durations
(a) Pre and post-light-dye Δ[HbT] time-course response to 12 seconds of stimulation averaged over n = 7 rats, runs = 5 per rat per condition, responses averaged per rat. Error bounds show SEM over rats (reproduced from Figure 3e). (b) Pre and post-light-dye Δ[HbT] responses to 2 seconds of hindpaw stimulation averaged over n = 5 rats, runs = 5 per rat per condition. Error bounds show SEM. Equivalent Δ[HbO] and Δ[HbR] traces are shown in supplemental figure S4 below. For (a) – (c), the region of interest was the same for all conditions and was centered over the responding region and included both arteries and parenchyma. Black bar: Stimulus duration, gray crosshairs: allow comparison of amplitudes in (a) and (b) at t = 2 seconds. (c-d) Δ[HbT] amplitudes for 12 and 2 second stimuli averaged over the "peak" (4-6 seconds) and "plateau" (10-12 seconds, c only) time periods, shown as a percentage of the pre-light-dye 2 and 12-second "peak" responses respectively (c reproduced from Figure 3f). Black dots: mean, boxes: SEM, whiskers: range of data. (e) Percent change in diameter of responding pial arteries pre and post-light-dye for 12-second "peak", 12-second "plateau" (n = 5 rats, 5 runs per rat per condition), and 2-second "peak" (n = 4 rats, runs = 15 per rat per condition). Diameters calculated from averages of 5 runs. Whiskers: SEM. P-values from Student's t test.

S4. HbO, HbR and HbT responses pre and post light-dye

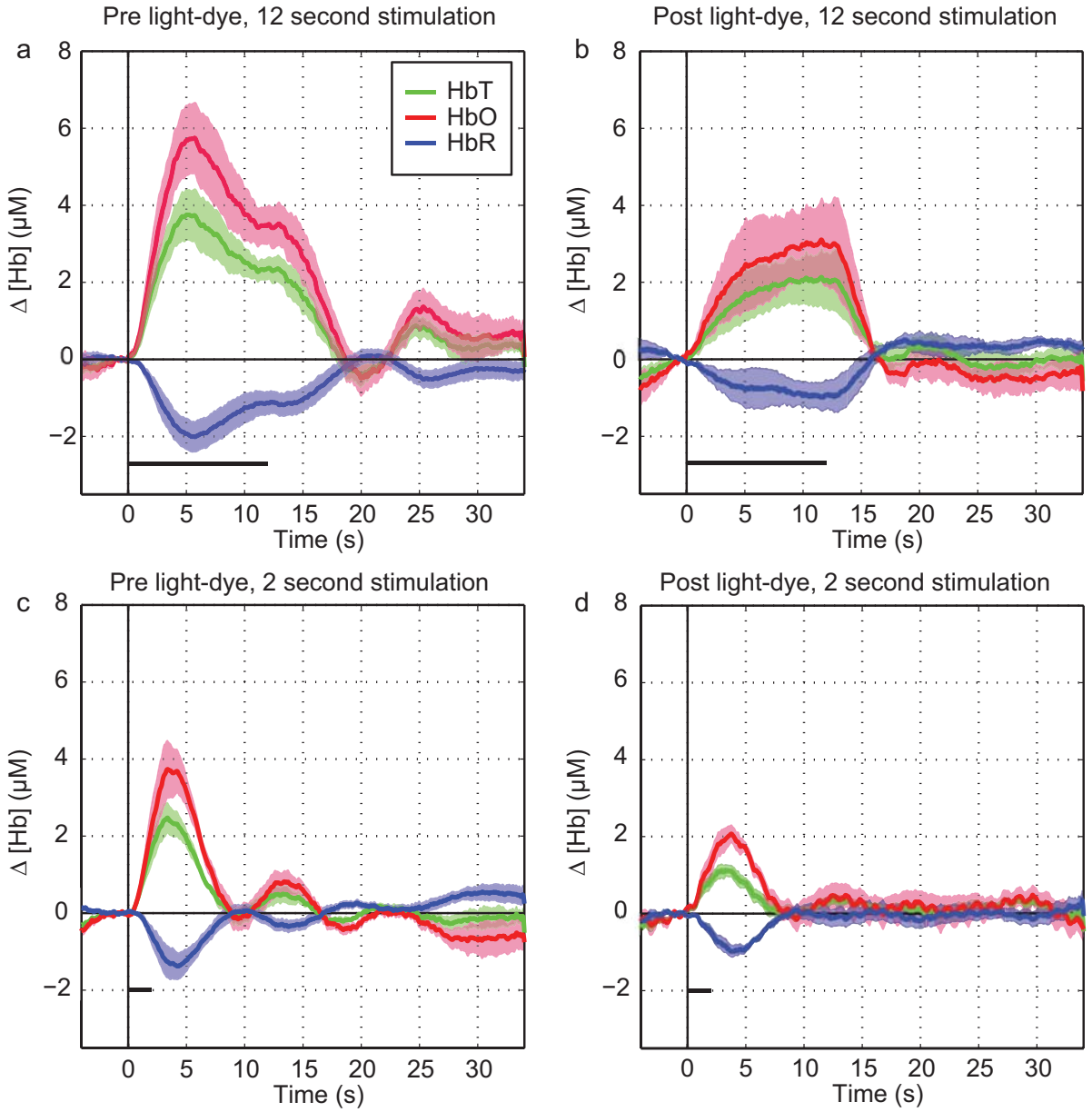

Figure S4. HbO, HbR and HbT responses pre and post light-dye treatment for 2 and 12 second stimuli (equivalent to HbT responses in Figure 2e). Recent work by Kennerley et al utilized maximal pre-dilation by hypercapnia in an attempt to impair stimulus-evoked arterial dilation in the somatosensory cortex[6]. Although the authors observed an almost identical residual response to somatosensory stimulation as we observed following light-dye treatment (Figure 3e), their manipulation evoked massive increases in baseline HbT (a 25 μM change from 104 μM to 129 μM), baseline flow and hyperoxia such that they observed no stimulus-evoked changes in ΔHbR. Their further observation of modified electrophysiological responses under these conditions led them to conclude that altered neuronal responses, and not elimination of arterial dilation, had modified their functional response. We found that light-dye treatment did not alter neuronal responses (Figure 4b-d), and that while light-dye treatment caused a 14.4 ± 3.6 μM increase in baseline [HbT] (n = 7 rats, 5 runs per rat), significant changes in HbR were observed following light-dye treatment (b and d above). We conclude that pre-dilation effects were not sufficient to induce hyperoxia. Error bounds show SEM across rats.

S5. Pre-dilation control

An increase in baseline arterial diameter could arguably reduce the capacity of the artery to dilate in response to stimulus. Increased baseline diameters also cause a local increase in baseline blood flow, and therefore oxygen and glucose delivery, which can potentially affect stimulus response mechanisms and even underlying neuronal activity itself.

To address whether the pre-dilation effect of our wide-field light-dye-treatment was sufficient to attenuate arterial dilations in response to stimulus, we induced local pre-dilation in surface arteries using topical application of 1-2μM Acetylcholine, ACh, and evaluated the ability of the vessels to respond to stimulation as a function of their baseline diameters. Control responses to 12 s stimulation were first recorded. The cranial window was then removed such that ACh could be applied to the exposed cortex. Immediately after ACh application, a layer of agarose was applied and the cranial window was re-sealed to minimize brain motion during imaging. ACh acts upon the endothelium to generate pre-dilation, and therefore like light-dye-treatment, should not alter the function of smooth muscle cells. After the application of ACh, pial arteries with resting diameters between 30-50 microns gradually dilated by up to 30 μm and eventually returned to their original baseline diameters over the course of approximately 1 hour. Throughout this period, hemodynamic responses to 12 second stimulation in the absence of any light-dye treatment were recorded.

The functional maps in Figure S5 reveal that contrary to the effects of light-dye-treatment, pre-dilation of pial arteries to an equivalent level of around +7-10 μm (20%) did not prevent stimulus-evoked dilation, nor did it affect the temporal shape of the response; leaving the initial peak and subsequent plateau of the response in place for pre-dilation levels less than +23 μm (Figure S5b). Even for pre-dilation levels greater than +20 μm, functional dilations of arterial branches were still observed. To summarize this data, we plot the amplitude of the peak Δ[HbT] responses observed across 3 rats as a function of their vessel's pre-dilation. Peak Δ[HbT] amplitudes are generally unaffected by increases in baseline diameters between 0 and +10 μm. At higher levels of pre-dilation, a gradual decrease in peak Δ[HbT] amplitude is seen as baseline diameters increase (Figure S5b-c). Equivalent results for our light-dye treatment measurements are plotted on the same axes and are found to be significantly different from this trend ($p < 0.0001$, Student's t test), suggesting that endothelial disruption, and not pre-dilation alone is responsible for light-dye-induced changes in functional hemodynamics (Figure 3).

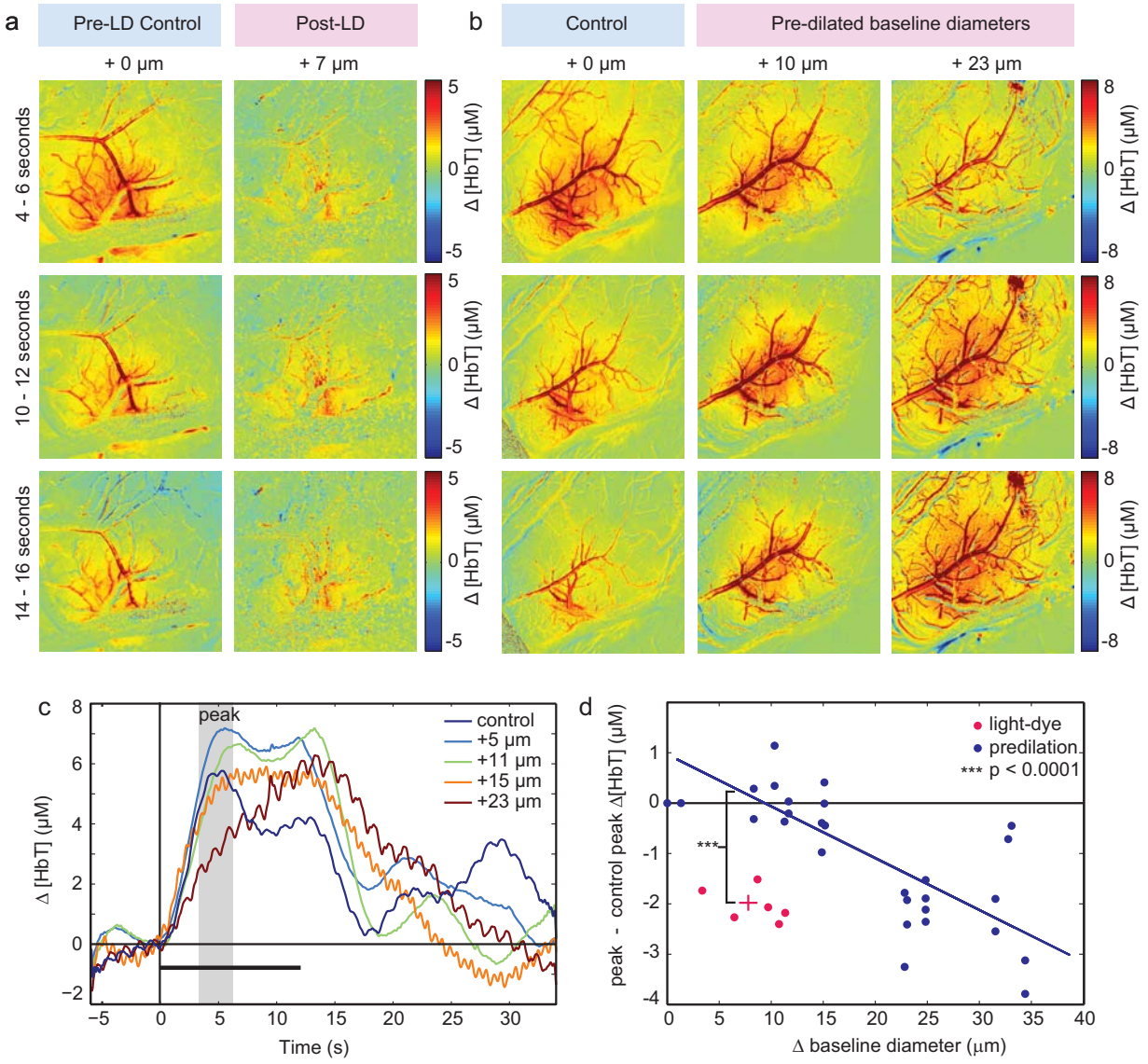

Figure S5. Pre-dilation does not significantly affect arterial responsiveness to stimulation (a). Functional maps showing pre-light-dye (control, left) and post-light-dye treatment (right) Δ[HbT] responses to 12 second stimulus averaged between 4-6 seconds (top), 10-12 seconds (middle), and 14-16 seconds (bottom) after stimulus onset. Post-light-dye functional maps lack dilation of pial arteries. (b) Functional maps showing Δ[HbT] response evolution when baseline diameters are pre-dilated using topical ACh by 0 µm (control), +10 µm, and +23 µm (left to right), all in the absence of light-dye treatment. Pial arterial responses are still observed, even in the presence of pre-dilated baseline diameters. (c) Δ[HbT] time-courses extracted from the same region in a single rat for increasing amounts of pre-dilation. (d) The change in peak Δ[HbT] amplitude (as indicated by gray region in (c)) relative to the control peak Δ[HbT] is plotted for varying degrees of induced baseline pre-dilation (blue dots, n = 3 rats, 10 measurements per rat) and for light-dye experiments (pink dots, n = 6 rats, 5 runs averaged per rat). The solid regression line is the ordinary least-squares fit to the pre-dilation data (with no light-dye). The pink cross shows the mean and SEM of both variables for the light-dye data. Our comparison tests whether there is an additional effect of light-dye on peak amplitudes (relative to the effect of pre-dilation alone) while controlling for the influence of baseline dilation. We implemented this multiple regression comparison using ordinary least squares by regressing peak amplitude on a constant, baseline diameter, and an indicator variable that is one if light-dye treatment is applied and is zero otherwise. We test the null hypothesis that light-dye treatment has no effect on peak amplitude beyond its effect of baseline diameter by examining the t-statistic for the coefficient on the indicator variable – we reject this null hypothesis ($p < 0.0001$, Student's t test).

S6. Temporal dynamics of the cortical response to SNP application

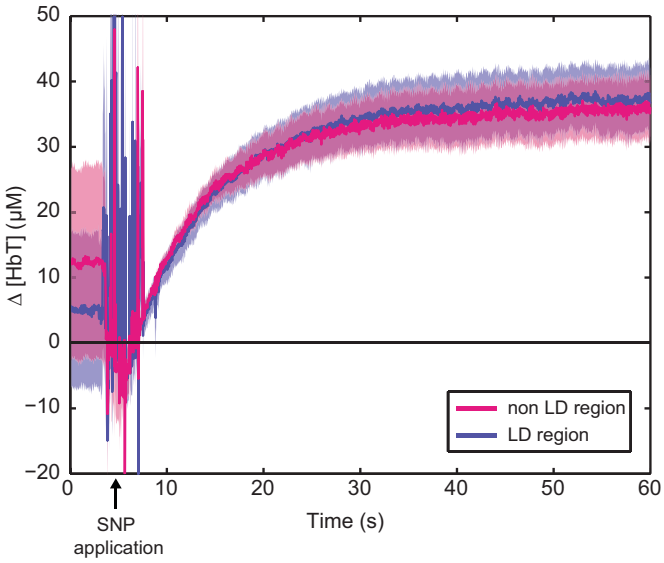

Figure S6. Temporal dynamics of the cortical response to SNP application. In addition to the response amplitude measures shown in Figure 4d, this plot shows that the dynamics of Δ[HbT] responses (as a measure of vasodilation) to topical application of SNP (0.□□□) remain the same in both non light-dye regions (blue) and light-dye treated regions (pink). This further confirms that vascular smooth muscle integrity was unaffected by light-dye treatment. Bold time-courses represent the average response over n = 5 rats, 1 observation per rat. Shaded regions show SEM.

Literature cited within supplemental material:

1. Tian P, Devor A, Sakadžić S, Dale AM, Boas DA. Monte Carlo simulation of the spatial resolution and depth sensitivity of two-dimensional optical imaging of the brain. *Journal of Biomedical Optics*. 2011;16:016006-016006-016013
2. Boyden ES, Zhang F, Bamberg E, Nagel G, Deisseroth K. Millisecond-timescale, genetically targeted optical control of neural activity. *Nature Neuroscience*. 2005;8:1263-1268
3. Aravanis AM, Wang L-P, Zhang F, Meltzer LA, Mogri MZ, Schneider MB, Deisseroth K. An optical neural interface: in vivo control of rodent motor cortex with integrated fiberoptic and optogenetic technology. *Journal of Neural Engineering*. 2007;4:S143
4. Yizhar O, Fenno Lief E, Davidson Thomas J, Mogri M, Deisseroth K. Optogenetics in Neural Systems. *Neuron*. 2011;71:9-34
5. Bernstein JG, Han X, Henninger MA, Ko EY, Qian X, Talei Franzesi G, McConnell JP, Stern P, Desimone R, Boyden ES. Prosthetic systems for therapeutic optical activation and silencing of genetically targeted neurons. 2008;6854:68540H-68540H-68511
6. Kennerley AJ, Harris S, Bruyns-Haylett M, Boorman L, Zheng Y, Jones M, Berwick J. Early and late stimulus-evoked cortical hemodynamic responses provide insight into the neurogenic nature of neurovascular coupling. *J Cereb Blood Flow Metab*. 2011

A Critical Role for the Vascular Endothelium in Functional Neurovascular Coupling in the Brain

Brenda R. Chen, Mariel G. Kozberg, Matthew B. Bouchard, Mohammed A. Shaik and Elizabeth M. C. Hillman

J Am Heart Assoc. 2014;3:e000787; originally published June 12, 2014;
doi: 10.1161/JAHA.114.000787
The *Journal of the American Heart Association* is published by the American Heart Association, 7272 Greenville Avenue, Dallas, TX 75231
Online ISSN: 2047-9980

Supplemental figures and supporting information

Contents

S1. Light-dye illumination penetration analysis

The blue light illumination used for light-dye treatment in our studies will be both scattered and absorbed within brain tissue. The light-dye effect depends on three parameters; the concentration of FITC within the vessel, the irradiance (mW / mm^2) of illumination and the duration of the exposure. The values chosen in our experiments were based on literature review and preliminary studies that assessed irradiance and duration of illumination that was adequate to result in disruption of endothelial signaling in pial arteries, while leaving smooth muscle function intact (and producing no measurable damage in other vessels). The values chosen were 5-6 minutes of exposure with irradiance of 488 or 473 nm light at the cortex of ~6 mW/mm^2. However, it is important for us to consider whether this illumination at the surface may have also affected vessels deeper within the cortex.

Fortunately, much attention in recent years has been paid to the propagation of blue light within the rodent cortex, since the light used for light-dye experiments is identical to that used in optogenetics studies [2]. In optogenetics, it is important to assess how far blue light penetrates into the brain before being attenuated to a point where it no longer meets the threshold for optogenetic excitation. In our case, these prior measurements and modeled values can provide insight into the action of light-dye.

Most measurements of blue light propagation in brain tissue have been performed in ex-vivo brain tissues [3]. This will likely over-estimate penetration of light, since in-vivo propagation of blue light will be strongly influenced by hemoglobin in this range. In our case, FITC is also present, which strongly absorbs at 473 and 488 nm. Optogenetic simulation geometries also generally assume a fiber optic illumination with specified fiber diameter, numerical aperture and distance between the fiber and brain. However, our illumination geometry can be readily modeled in these terms, with our 'wide-field' illumination being equivalent to a ~1,000 micron diameter fiber with low NA (e.g. 0.01) in contact with the brain's surface, while our 'light-line' illumination (along its focused axis) would be equivalent to a 0.025 NA fiber with a 50 micron diameter also in contact with the tissue.

A model based on Kubelka-Munk theory (ignoring contributions from absorption) predicts Figure S1, which shows the intracortical irradiance for each of these geometries (assuming S = 10.3 mm^{-1} for rat brain, measured in [3]).

This very conservative estimate (since this model is based on brain slice measurements with no absorbing blood or FITC present) suggests that the irradiance reduces to 50% at a depth of around 100 microns, and to around 10% at a depth of 400 microns. Our light-line geometry is slightly more superficially weighted. These estimates are consistent with a number of other studies using empirical measurements and Monte Carlo simulations [4,5].

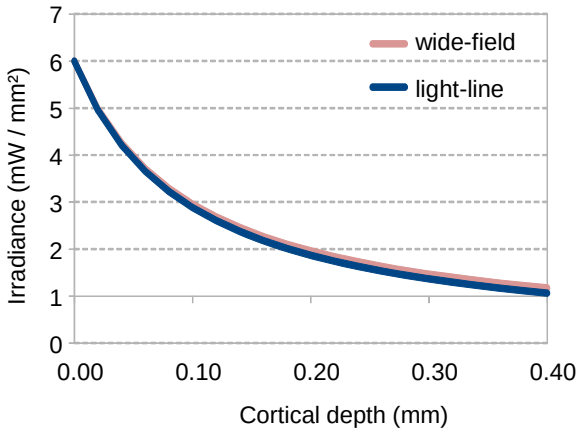

Figure S1. Calculated intensity of 488 nm blue light in the rat cortex as a function of depth for our two different light-dye geometries.

While quantification of the exact irradiance threshold for light-dye treatment is difficult to discern, we certainly noted in our original experiments that reducing either illumination or duration of exposure by half failed to achieve the endothelium-disruption effect of light-dye treatment. We therefore estimate that the action of

our light-dye experiments was constrained to vasculature within the top 100-200 microns of the cortex. As illustrated in figure S2 below, this depth will mostly affect pial arteries and the top segments of diving arterioles, but deeper arterioles likely maintain their function.

S2. Depth sensitivity and interpretation of MS-OISI

Similar analysis to that presented above can also be used to understand the meaning and origin of cortical signals observed using MS-OISI. A recent, detailed paper by Tian et al directly addressed this issue using Monte Carlo simulations of the sensitivity of visible light to cortical changes in absorption [1]. It should be noted that the level of light penetration (shown above) is not the same as a sensitivity measure, since the light detected by a camera must travel back out of the tissue before being detected. Parameters such as the lateral size of the responding region and the numerical aperture of the detection optics therefore also play a role in governing depth sensitivity. However, analyzing these variables, Tian et al showed that at 633 nm, absorption changes occurring at a depth between 200-300 microns contribute around 15% to the total detected signal, compared to ~32% for equivalent changes occurring in the top 100 microns, and ~5% from changes originating at depths between 300-400 microns (~ layer III). The study also demonstrates the 'blurring' effect of depth, such that a small, laterally discrete region at a depth of 400 microns would have a spatial resolution of 100-300 microns. In practice, this explains why individual capillaries or other sub-pial vessels cannot be spatially resolved, however, they do contribute substantially to the MS-OISI signals detected at the superficial cortex. Since superficial vessels are only very minimally blurred, and since the structure of the cortical vasculature is laid out to have all of the horizontally traveling pial vessels at the surface, this capillary / diving vessel signal can be discerned from signal changes seen in-between pial vessels. This is illustrated schematically in figure S2 below.

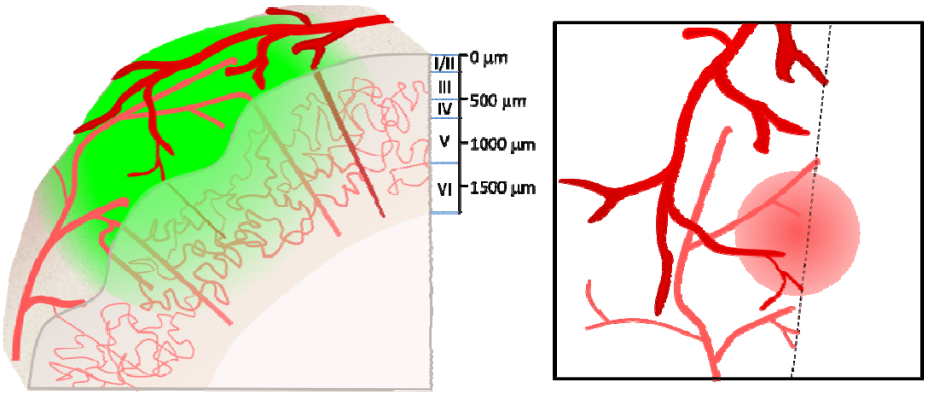

Figure S2. The spatial sensitivity and resolution of MS-OISI. Left: 3D schematic of the rodent cortex showing surface illumination with green light. The cross-sectional vascular organization of the cortex means that most large vessels are located on the pial surface, with diving arterioles and venules feeding deeper capillary beds. Right: sketch of the same section of cortex viewed en-face by MS-OISI (dotted line illustrates cut-through section shown left). Surface vessels appear strong and sharp. Contributions from changes in deeper capillary beds and diving vessels contribute to the more diffuse background signal seen in the 'parenchyma'.

S3. Comparison of 12 and 2 second stimulus duration pre/post light-dye

The pre- and post-LD response for 2 second stimulation show identical time-courses to the 12 second stimulation up to t = 2 seconds. After cessation of the 2 second stimulus, the post-LD response begins to return to baseline slightly before the pre-LD response. Considering the response magnitude as the area under each curve, wide-field light-dye treatment targeting pial arteries appears to have a larger net effect on the hemodynamic response to shorter stimuli. This is consistent with endothelial hyperpolarization dominating the early phase of the response.

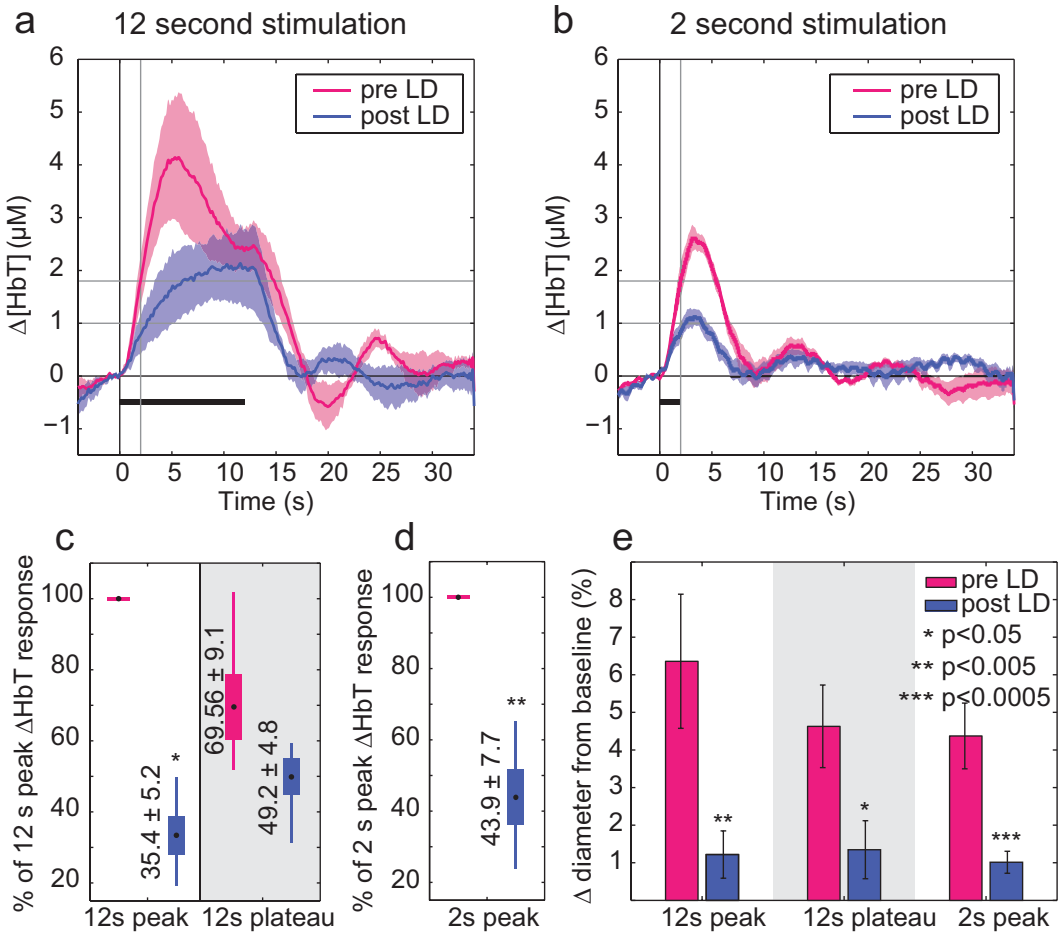

Figure S3. Comparison of the effect of wide-field light-dye treatment for 12 and 2 second stimulus durations
(a) Pre and post-light-dye Δ[HbT] time-course response to 12 seconds of stimulation averaged over n = 7 rats, runs = 5 per rat per condition, responses averaged per rat. Error bounds show SEM over rats (reproduced from Figure 3e). (b) Pre and post-light-dye Δ[HbT] responses to 2 seconds of hindpaw stimulation averaged over n = 5 rats, runs = 5 per rat per condition. Error bounds show SEM. Equivalent Δ[HbO] and Δ[HbR] traces are shown in supplemental figure S4 below. For (a) – (c), the region of interest was the same for all conditions and was centered over the responding region and included both arteries and parenchyma. Black bar: Stimulus duration, gray crosshairs: allow comparison of amplitudes in (a) and (b) at t = 2 seconds. (c-d) Δ[HbT] amplitudes for 12 and 2 second stimuli averaged over the "peak" (4-6 seconds) and "plateau" (10-12 seconds, c only) time periods, shown as a percentage of the pre-light-dye 2 and 12-second "peak" responses respectively (c reproduced from Figure 3f). Black dots: mean, boxes: SEM, whiskers: range of data. (e) Percent change in diameter of responding pial arteries pre and post-light-dye for 12-second "peak", 12-second "plateau" (n = 5 rats, 5 runs per rat per condition), and 2-second "peak" (n = 4 rats, runs = 15 per rat per condition). Diameters calculated from averages of 5 runs. Whiskers: SEM. P-values from Student's t test.

S4. HbO, HbR and HbT responses pre and post light-dye

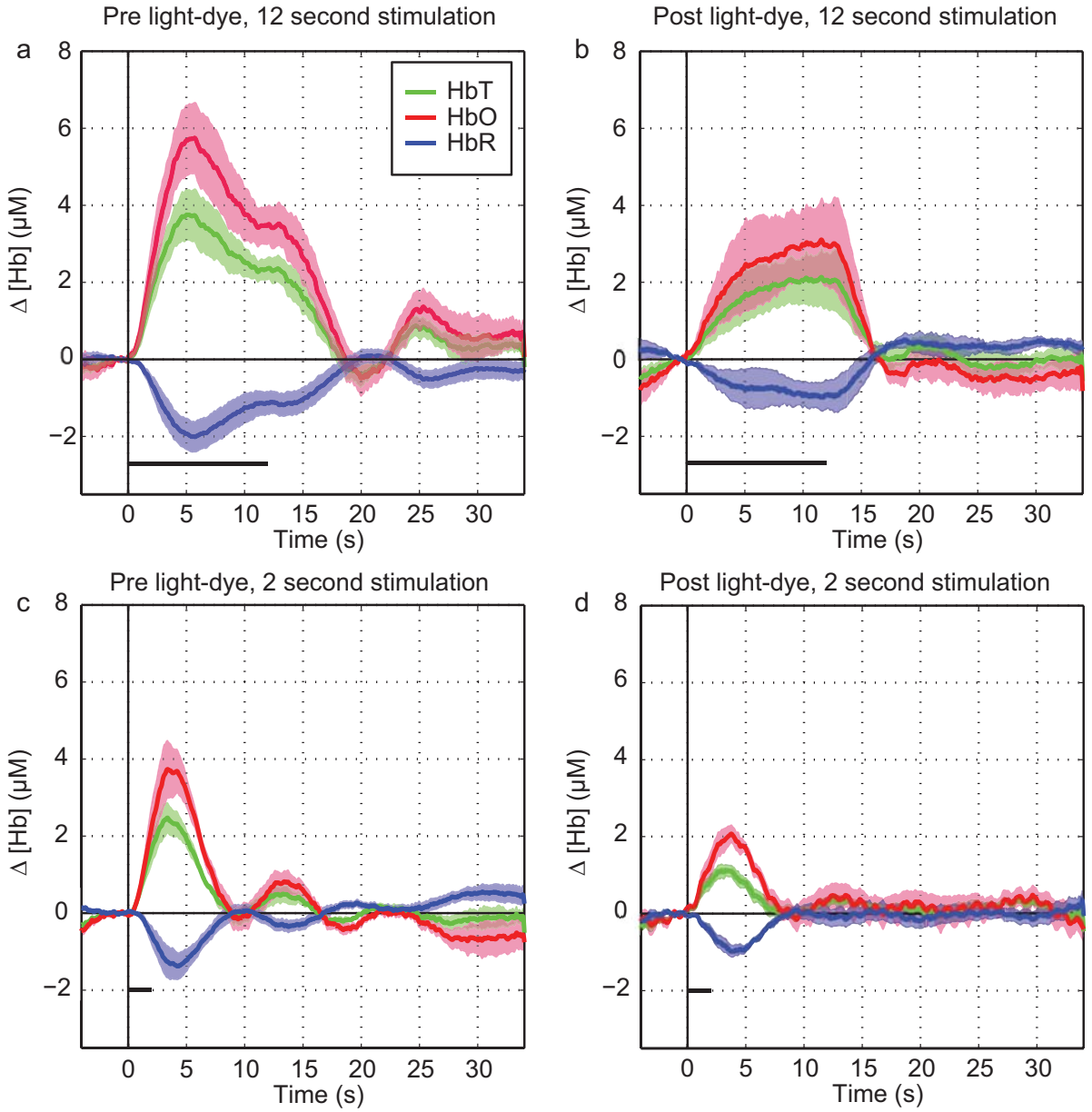

Figure S4. HbO, HbR and HbT responses pre and post light-dye treatment for 2 and 12 second stimuli (equivalent to HbT responses in Figure 2e). Recent work by Kennerley et al utilized maximal pre-dilation by hypercapnia in an attempt to impair stimulus-evoked arterial dilation in the somatosensory cortex[6]. Although the authors observed an almost identical residual response to somatosensory stimulation as we observed following light-dye treatment (Figure 3e), their manipulation evoked massive increases in baseline HbT (a 25 μM change from 104 μM to 129 μM), baseline flow and hyperoxia such that they observed no stimulus-evoked changes in ΔHbR. Their further observation of modified electrophysiological responses under these conditions led them to conclude that altered neuronal responses, and not elimination of arterial dilation, had modified their functional response. We found that light-dye treatment did not alter neuronal responses (Figure 4b-d), and that while light-dye treatment caused a 14.4 ± 3.6 μM increase in baseline [HbT] (n = 7 rats, 5 runs per rat), significant changes in HbR were observed following light-dye treatment (b and d above). We conclude that pre-dilation effects were not sufficient to induce hyperoxia. Error bounds show SEM across rats.

S5. Pre-dilation control

An increase in baseline arterial diameter could arguably reduce the capacity of the artery to dilate in response to stimulus. Increased baseline diameters also cause a local increase in baseline blood flow, and therefore oxygen and glucose delivery, which can potentially affect stimulus response mechanisms and even underlying neuronal activity itself.

To address whether the pre-dilation effect of our wide-field light-dye-treatment was sufficient to attenuate arterial dilations in response to stimulus, we induced local pre-dilation in surface arteries using topical application of 1-2μM Acetylcholine, ACh, and evaluated the ability of the vessels to respond to stimulation as a function of their baseline diameters. Control responses to 12 s stimulation were first recorded. The cranial window was then removed such that ACh could be applied to the exposed cortex. Immediately after ACh application, a layer of agarose was applied and the cranial window was re-sealed to minimize brain motion during imaging. ACh acts upon the endothelium to generate pre-dilation, and therefore like light-dye-treatment, should not alter the function of smooth muscle cells. After the application of ACh, pial arteries with resting diameters between 30-50 microns gradually dilated by up to 30 μm and eventually returned to their original baseline diameters over the course of approximately 1 hour. Throughout this period, hemodynamic responses to 12 second stimulation in the absence of any light-dye treatment were recorded.

The functional maps in Figure S5 reveal that contrary to the effects of light-dye-treatment, pre-dilation of pial arteries to an equivalent level of around +7-10 μm (20%) did not prevent stimulus-evoked dilation, nor did it affect the temporal shape of the response; leaving the initial peak and subsequent plateau of the response in place for pre-dilation levels less than +23 μm (Figure S5b). Even for pre-dilation levels greater than +20 μm, functional dilations of arterial branches were still observed. To summarize this data, we plot the amplitude of the peak Δ[HbT] responses observed across 3 rats as a function of their vessel's pre-dilation. Peak Δ[HbT] amplitudes are generally unaffected by increases in baseline diameters between 0 and +10 μm. At higher levels of pre-dilation, a gradual decrease in peak Δ[HbT] amplitude is seen as baseline diameters increase (Figure S5b-c). Equivalent results for our light-dye treatment measurements are plotted on the same axes and are found to be significantly different from this trend ($p < 0.0001$, Student's t test), suggesting that endothelial disruption, and not pre-dilation alone is responsible for light-dye-induced changes in functional hemodynamics (Figure 3).

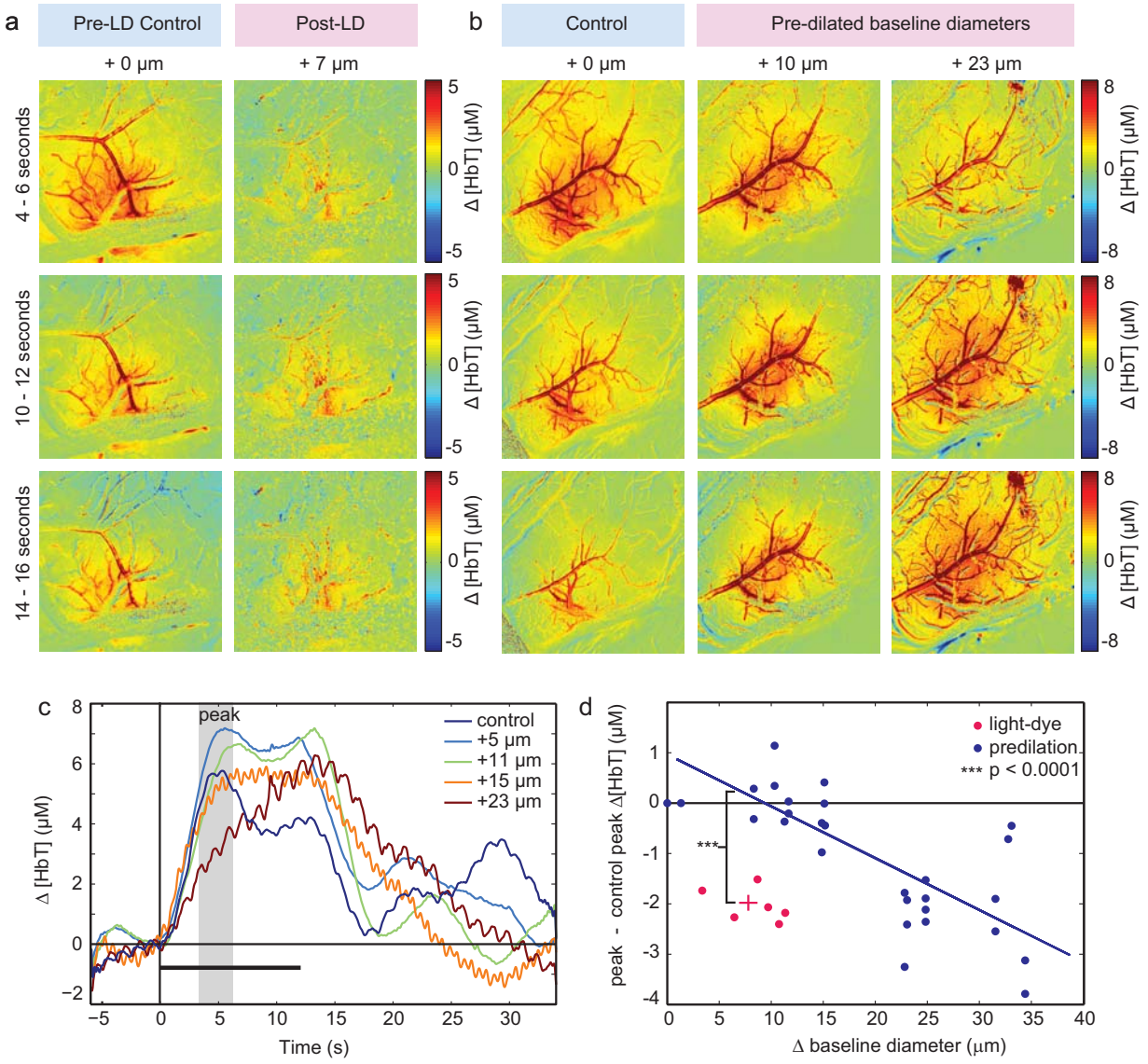

Figure S5. Pre-dilation does not significantly affect arterial responsiveness to stimulation (a). Functional maps showing pre-light-dye (control, left) and post-light-dye treatment (right) Δ[HbT] responses to 12 second stimulus averaged between 4-6 seconds (top), 10-12 seconds (middle), and 14-16 seconds (bottom) after stimulus onset. Post-light-dye functional maps lack dilation of pial arteries. (b) Functional maps showing Δ[HbT] response evolution when baseline diameters are pre-dilated using topical ACh by 0 µm (control), +10 µm, and +23 µm (left to right), all in the absence of light-dye treatment. Pial arterial responses are still observed, even in the presence of pre-dilated baseline diameters. (c) Δ[HbT] time-courses extracted from the same region in a single rat for increasing amounts of pre-dilation. (d) The change in peak Δ[HbT] amplitude (as indicated by gray region in (c)) relative to the control peak Δ[HbT] is plotted for varying degrees of induced baseline pre-dilation (blue dots, n = 3 rats, 10 measurements per rat) and for light-dye experiments (pink dots, n = 6 rats, 5 runs averaged per rat). The solid regression line is the ordinary least-squares fit to the pre-dilation data (with no light-dye). The pink cross shows the mean and SEM of both variables for the light-dye data. Our comparison tests whether there is an additional effect of light-dye on peak amplitudes (relative to the effect of pre-dilation alone) while controlling for the influence of baseline dilation. We implemented this multiple regression comparison using ordinary least squares by regressing peak amplitude on a constant, baseline diameter, and an indicator variable that is one if light-dye treatment is applied and is zero otherwise. We test the null hypothesis that light-dye treatment has no effect on peak amplitude beyond its effect of baseline diameter by examining the t-statistic for the coefficient on the indicator variable – we reject this null hypothesis ($p < 0.0001$, Student's t test).

S6. Temporal dynamics of the cortical response to SNP application

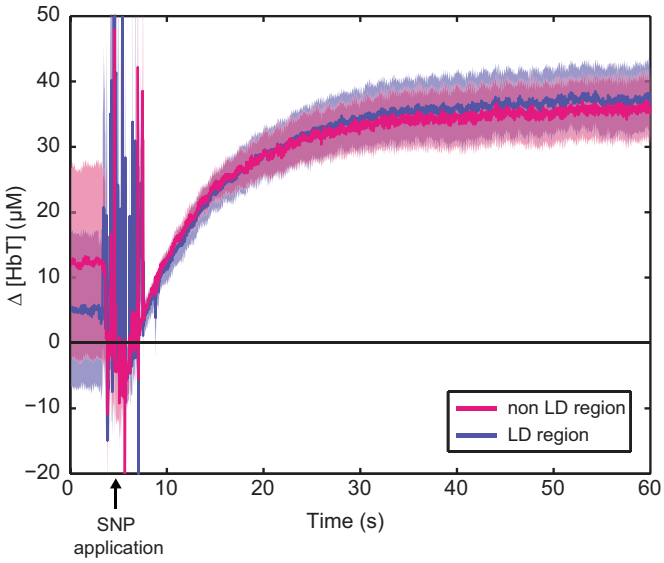

Figure S6. Temporal dynamics of the cortical response to SNP application. In addition to the response amplitude measures shown in Figure 4d, this plot shows that the dynamics of Δ[HbT] responses (as a measure of vasodilation) to topical application of SNP (0.□□□) remain the same in both non light-dye regions (blue) and light-dye treated regions (pink). This further confirms that vascular smooth muscle integrity was unaffected by light-dye treatment. Bold time-courses represent the average response over n = 5 rats, 1 observation per rat. Shaded regions show SEM.

Literature cited within supplemental material:

1. Tian P, Devor A, Sakadžić S, Dale AM, Boas DA. Monte Carlo simulation of the spatial resolution and depth sensitivity of two-dimensional optical imaging of the brain. *Journal of Biomedical Optics*. 2011;16:016006-016006-016013
2. Boyden ES, Zhang F, Bamberg E, Nagel G, Deisseroth K. Millisecond-timescale, genetically targeted optical control of neural activity. *Nature Neuroscience*. 2005;8:1263-1268
3. Aravanis AM, Wang L-P, Zhang F, Meltzer LA, Mogri MZ, Schneider MB, Deisseroth K. An optical neural interface: in vivo control of rodent motor cortex with integrated fiberoptic and optogenetic technology. *Journal of Neural Engineering*. 2007;4:S143
4. Yizhar O, Fenno Lief E, Davidson Thomas J, Mogri M, Deisseroth K. Optogenetics in Neural Systems. *Neuron*. 2011;71:9-34
5. Bernstein JG, Han X, Henninger MA, Ko EY, Qian X, Talei Franzesi G, McConnell JP, Stern P, Desimone R, Boyden ES. Prosthetic systems for therapeutic optical activation and silencing of genetically targeted neurons. 2008;6854:68540H-68540H-68511
6. Kennerley AJ, Harris S, Bruyns-Haylett M, Boorman L, Zheng Y, Jones M, Berwick J. Early and late stimulus-evoked cortical hemodynamic responses provide insight into the neurogenic nature of neurovascular coupling. *J Cereb Blood Flow Metab*. 2011